Metal–Oxo Complexes

International Edition: DOI: 10.1002/anie.201600507
German Edition: DOI: 10.1002/ange.201600507

Oxidation Reactions with Bioinspired Mononuclear Non-Heme Metal–Oxo Complexes

*Xenia Engelmann, Inés Monte-Pérez, and Kallol Ray**

Keywords:
C–H bond activation · copper · iron · manganese · metal–oxo complexes

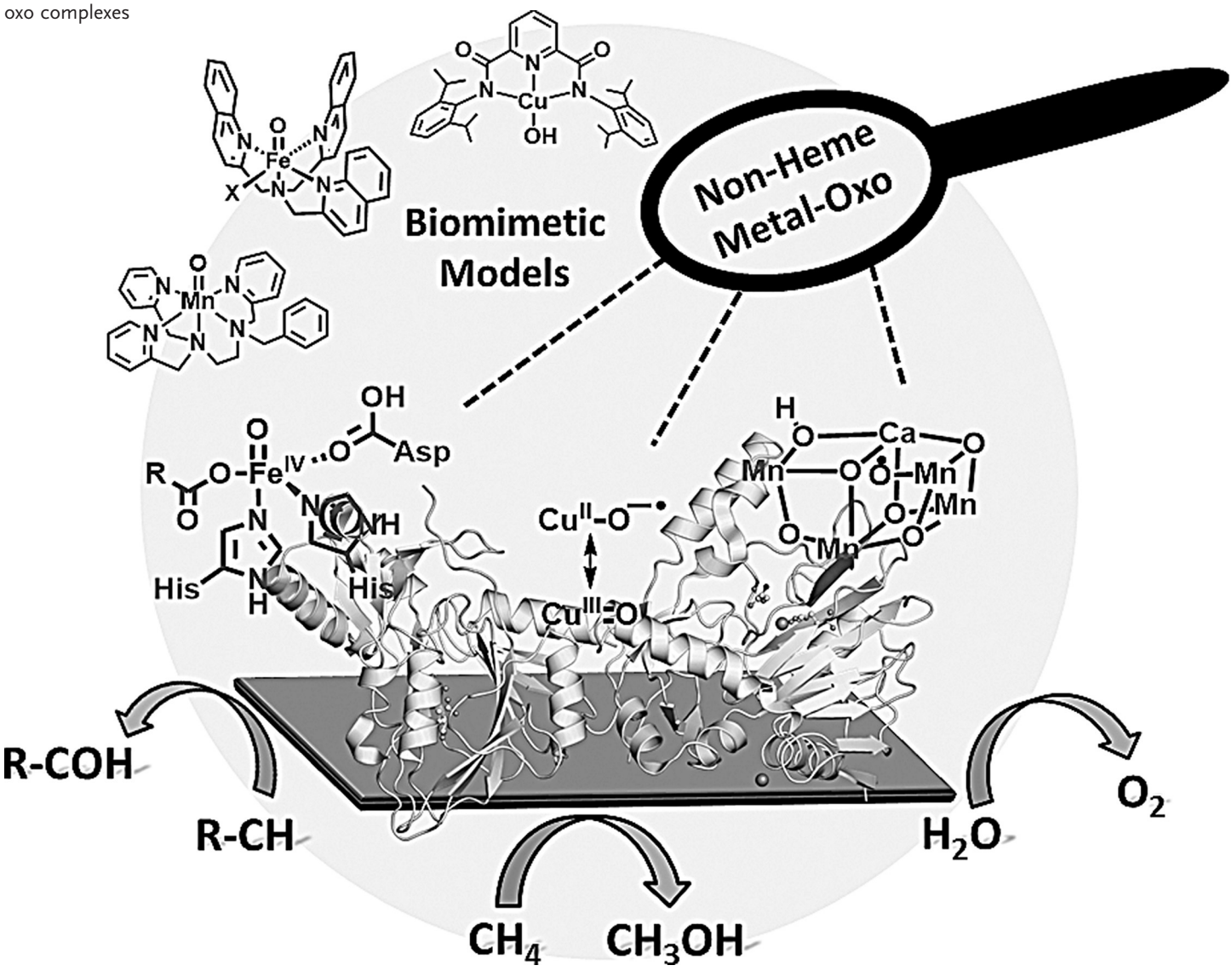

The selective functionalization of strong C–H bonds and the oxidation of water by cheap and nontoxic metals are some of the key targets of chemical research today. It has been proposed that high-valent iron-, manganese-, and copper-oxo cores are involved as reactive intermediates in important oxidation reactions performed by biological systems, thus making them attractive targets for biomimetic synthetic studies. The generation and characterization of metal–oxo model complexes of iron, manganese, and copper together with detailed reactivity studies can help in understanding how the steric and electronic properties of the metal centers modulate the reactivity of the metalloenzymes. This Review provides a focused overview of the advances in the chemistry of biomimetic high-valent metal–oxo complexes from the last 5–10 years that can be related to our understanding of biological systems.

From the Contents

1. Introduction

For decades, scientists have been searching for efficient and cheap catalysts for water splitting and selective oxidation reactions of hydrocarbons under ambient conditions, with the aim of finding alternative energy carriers to fossil-based oil for energy-conversion processes. Splitting water to generate molecular hydrogen and oxygen is an environmentally friendly method to convert solar energy.[1] The oxygen evolution reaction (OER) has been regarded as a rate-limiting step in realizing a fully integrated water-splitting system because of the high energy barrier for the metal–oxo mediated O–O bond-formation processes.[2] Precious-metal oxides, such as RuO_2 and IrO_2, exhibit superb catalytic activity in the OER;[3] however, their high price remains a disadvantage. Therefore, the development of efficient, durable, and inexpensive alternative catalysts is desirable.

The same is true for the conversion of methane into methanol. Although natural gas is a reasonable source of energy, its production and use are strongly limited by the difficulties in transporting it. Clearly, new catalyst technologies for the conversion of methane (the major component of natural gas) into methanol (a liquid) under moderate temperature and pressure could dramatically alter the scale and efficiency by which natural gas can be utilized.[4] The most efficient catalyst known so far is the platinum-based Periana catalyst, the industrial application of which is again limited because of the high cost of platinum together with the difficulties associated with the extraction of methanol from the reaction mixture.[5] Alternative energy resources also include biofuels, which are available from currently plentiful and renewable biomass.[6] Abundant biopolymers such as cellulose, chitin, lignin, and starches provide us with potential future sources of primary feedstock for the production of fuels.[7] Moreover, hydrolytic reactions by enzymes or under extreme chemical conditions, such as heating with sulfuric acid,[8] can also lead to useful breakdown products. Therefore, the generation of new classes of chemical catalysts which can effect biopolymer breakdown through oxidative reactions is also of tremendous technological importance.

Nature has used metalloenzymes for the selective functionalization of strong C–H bonds as well as the oxidation of water in atom-economical transformations that employ cheap and nontoxic metals and operate under ambient pressure and temperature. High-valent metal–oxo cores have been proposed, and in a few cases isolated, as the common reactive intermediates in these biological reactions relevant to the formation of renewable energy (Figure 1).[9] For example, a transient, but not yet isolated, manganese-oxo (Figure 1a) intermediate is proposed to be involved in the energy-demanding O–O bond-formation step, which is considered to be the most critical part of the evolution of dioxygen in photosystem II.[2,10]

Similarly, iron-oxo species have been found to be key oxidizing intermediates in the mechanisms of mononuclear iron enzymes (Figure 1b): high-valent iron-oxo intermediates have now been trapped and spectroscopically characterized in a number of heme and non-heme enzymes and shown to be responsible for a variety of oxidative transformations, including hydroxylation, halogenation, desaturation, and formation of heterocylic rings.[9a–c] Furthermore, a bis(μ-oxo)diiron(IV) intermediate Q (Figure 1c) has been trapped in the catalytic cycle of the soluble methane monooxygenase (sMMO),[11,12] and demonstrated to be kinetically competent at hydroxylating methane. Inspired by the mechanism of the iron-mediated biological oxidation reactions, high-valent copper-oxo cores (Figure 1d) have also been implicated as reactive intermediates in copper-mediated biological oxidation reactions.[9a,13] Many proposals have appeared for the involvement of $[CuO]^+$ species, as well as the protonated version $[Cu(OH)]^{2+}$,[13a] during the C–H oxidative cleavage of biopolymers and other substrates at the active sites of mononuclear (in lytic polysaccharide monooxygenases; LPMO)[14] as well as noncoupled dicopper (in dopamine β-monooxygenase (DβM) and peptidylglycine α-amidating monooxygenase

[*] X. Engelmann, I. Monte-Pérez, Prof. Dr. K. Ray
Department of Chemistry, Humboldt-Universität zu Berlin
Brook-Taylor-Strasse 2, 12489 Berlin (Germany)
E-mail: kallol.ray@chemie.hu-berlin.de

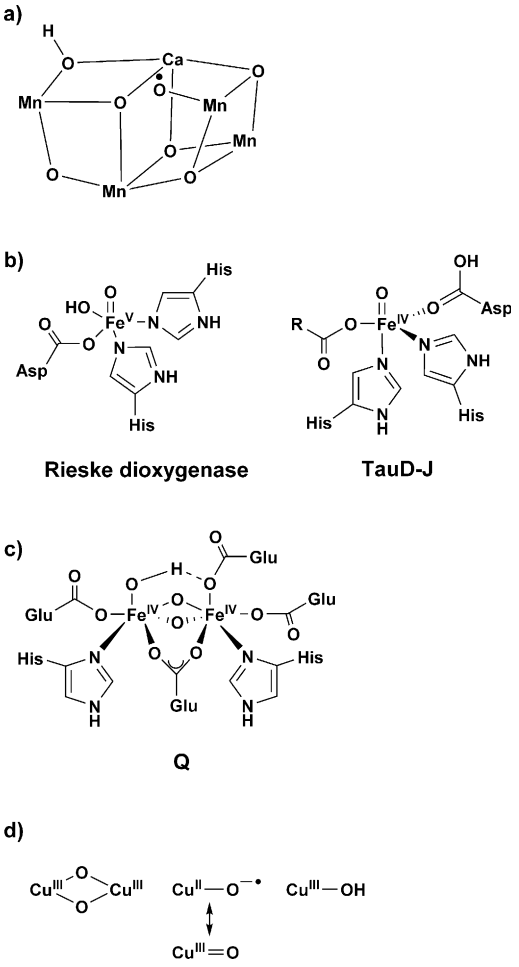

Figure 1. The structures of high-valent metal–oxo intermediates in non-heme enzymatic systems: a) Structure of the oxygen-evolving complex showing the proposed Mn^{IV}-oxyl core involved in the O–O bond-formation process; b) mononuclear iron-oxo species involved in the catalytic cycles of taurine dioxygenase (TauD) and rieske dioxygenase enzymes; c) intermediate Q of soluble methane monooxygenase; d) proposed copper-oxo/hydroxo reactive intermediates in the catalytic cycles of copper-containing oxygenases.

(PHM)) metalloenzymes.[15] However, supporting evidence is sparse and indirect, and such species have not been observed directly as discrete intermediates during catalysis.[9a,16] The involvement of bis(μ-oxo)dicopper(III) cores in biological C–H bond hydroxylation reactions has also been controversially discussed in the literature. Although, such a species has been suggested as an intermediate which may form at the dicopper active site in particulate methane monooxygenase (pMMO) and effect methane oxygenation chemistry,[13h] the Cu^{III} oxidation state is yet to be assigned definitively to any redox mechanism in biology.[13b] Research efforts in current bioinorganic chemistry are, therefore, dedicated toward the identity of LPMO, DβM, PHM, and pMMO oxygenated intermediates and the mechanism by which strong C–H bonds are activated.[16]

Gaining an understanding of the structure–function relationships of the metalloenzymes will not only be of great interest in its own right, but may also aid the development of artificial catalysts that are as efficient as the enzymes and are based on inexpensive and abundant materials. Furthermore, to engineer improved catalysts, there is a substantial impetus to fully characterize the active species, including all relevant high oxidation states, intermediates, and transition states, to establish the mechanism(s) by which oxidation reactions are carried out in biology. However, biological intermediates are short-lived and highly reactive in most cases, thus making it difficult to study their chemical and physical properties in the catalytic cycles of metalloenzymes. The proposed involvement of high-valent manganese-, iron-, and copper-oxo cores in biological oxidation reactions have, therefore, made them attractive targets for biomimetic synthetic studies. Indeed, recent synthetic advances have led to the isolation and characterization of several well-characterized metal–oxo model complexes of Mn, Fe, and Cu; detailed reactivity studies in conjunction with spectroscopy and theory have helped to understand how the steric and electronic properties of the metal centers modulate their reactivity.[9a,c,13e,16,17] Although the synthesized complexes have been found to be reactive toward substrates containing weak C–H bonds, in most cases the exhibited reactions are moderate and noncatalytic, with activities falling far short of the activity of the biological catalysts. Moreover, only in extremely rare cases are they found to be efficient in initiating O–O bond formation. Current issues in bioinorganic chemistry are, therefore, associated with obtaining a proper understanding of the factors that lead to the enhanced reactivity of the model metal–oxo complexes and the design of artificial

Xenia Engelmann was born in Berlin. She studied chemistry at the Humboldt-Universität zu Berlin and received her MSc in chemistry in 2015. She is currently working in the group of Prof. Dr. Kallol Ray on biomimetic dioxygen activation reactions involving first row transition metals.

Inés Monte Pérez was born in Mexico City. She studied chemistry at the National Autonomous University of México, where she obtained her MSc in 2012. Currently, she is working at the Humboldt-Universität zu Berlin under the supervision of Prof. Kallol Ray on the synthesis and characterization of reactive intermediates, with a focus on iron-oxo and copper-nitrene systems.

systems that parallel the reactivity of the biological catalysts. In this Review, milestones from the last 5–10 years of mononuclear non-heme chemistry will be discussed.

2. Reactivity of Metal–Oxo Complexes

The majority of the catalytic reactions performed by the metal–oxo (M^n=O) complexes involve either a C–H activation process or an oxygen atom transfer (OAT) reaction. From studies on high-valent heme complexes,[18] the mechanism through which C–H bonds are oxidized by non-heme metal–oxo complexes can be construed to involve a rate-determining hydrogen atom abstraction (HAA) reaction. Although the oxo transfer reactions are predominantly controlled by the M^n=O/M^{n-1}=O redox couple, the HAA ability of the metal–oxo cores can be viewed within the context of studies carried out by Mayer and co-workers.[19] They showed that the rates of toluene oxidation by a series of oxygen-centered oxidants did not depend on the amount of radical character associated with the oxygen atom of the oxidant, but instead correlated linearly with the strength of the O–H bond formed upon reduction of the oxidant [D(O-H); Eq. (1), (where C is a constant).[19a–c]

$$D(\mathrm{O\text{-}H}) = 23.06\,E_{1/2} + 1.32\,\mathrm{p}K_a + C \quad (1)$$

For HAA reactions involving transition-metal ions, where the electrons and protons are often substantially separated, the spin density is even more distantly connected to reactivity.[19d] For example, C–H activation reactions mediated by metal–oxo cores, where the electrons and protons are transferred to separated sites (the proton to the oxo group and the electron to the metal ion through a concerted proton and electron transfer mechanism (CPET); Scheme 1), emphasized the importance of the Bordwell/Polanyi[20] relationship in determining the thermodynamic affinity of HAA reactions. This affinity (D(O-H) in kcal mol^{-1}) is equivalent to the affinity of the oxidized metal–oxo species for an electron (redox potential $E_{1/2}$ in V for the M^n=O/M^{n-1}=O couple) and the affinity of the reduced metal–oxo species for a proton (acid dissociation constant K_a of the conjugate base M^{n-1}–OH), because a hydrogen atom is equivalent to $H^+ + e^-$ (see the thermodynamic cycle shown in Scheme 1).

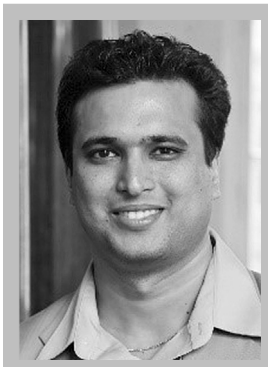

Kallol Ray studied chemistry at the University of Kolkata (India). After obtaining his MSc at the Indian Institute of Technology (Kanpur, 2001), he received his PhD with Prof. Dr. Karl Wieghardt at the Max-Planck Institute of Bioinorganic Chemistry (Mülheim/Ruhr) and Ruhr-University Bochum (2005). He then conducted postdoctoral research on high-valent oxoiron(IV) complexes with Prof. Lawrence Que, Jr. at the University of Minnesota (USA). In 2009, he joined the Humboldt-Universität zu Berlin as a junior research group leader within the Cluster of Excellence, Unifying Concepts in Catalysis (UniCat, Berlin).

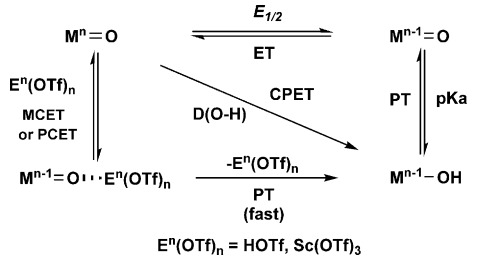

Scheme 1. Thermodynamic cycle describing the affinity of a metal–oxo species for concerted proton and electron transfers (CPET), stepwise proton and electron transfers (PT/ET), and uncoupled metal/proton-assisted electron transfer (MCET/PCET) followed by a fast proton transfer. D(O-H) is the strength of the O–H bond of M^{n-1}–OH [Eq. (1)].

Insights into the oxidative reactivity of the M=O moiety can also be derived from considerations of simple ligand-field theory.[16] The energetic ordering of the d orbitals $d_{xy} < d_{xz,yz} < d_{x^2-y^2} < d_{z^2}$ in C_{4v} symmetry, is a consequence of the tetragonal compression associated with the strong M=O bond (see Figure 2a for an Fe^{IV}=O species). Whereas the $d_{x^2-y^2}$ and d_{z^2} orbitals form strongly antibonding combinations with the σ orbitals of the ligands, the d_{xz} and d_{yz} orbitals result in antibonding π* orbitals by interacting with the p_x and p_y orbitals of the oxo ligand. The key frontier molecular orbitals (FMOs) that are likely to be involved in the HAA and OAT steps are the π* $d_{xz/yz}$ and the σ* d_{z^2} orbitals. The transfer of a hydrogen atom from the σ(C–H) orbital to the M=O species (solid arrows; Figure 2a) will result in protonation of the oxo atom and the introduction of a single electron into either a σ* or a π* orbital of M=O. The exact nature of the electron acceptor orbital will depend on the relative energies of the d_{z^2} and $d_{xz/yz}$ orbitals, which will be controlled by the nature of the supporting ligand and the covalency of the M=O bond.

The different requirements for the optimal interaction between the electron acceptor and electron donor orbitals also induces different steric requirements for the σ and π pathways.[13l] To maximize the overlap between the d_{z^2} and the σ_{CH} orbitals in the case of the σ pathway (Figure 2a), the system directs a vertical approach of the target C–H bond towards the M=O core, thereby leading to a linear M-O-H angle. In contrast, the π channel involving $d_{xz,yz}$-based electron acceptor orbitals typically exhibits a bent M-O-H angle. The steric interaction between the substrates and metal chelates as directed by the FMOs associated with the HAA step will, therefore, be of great importance in controlling the reactivity of metal–oxo cores toward C–H bonds.

For the OAT process, on the other hand, two electrons need to be transferred simultaneously to the σ* and π* orbitals of the M=O core (dashed arrows; Figure 2a), and a similar steric consideration (as in the HAA process) will not be applicable. The OAT and HAA reactivities of M=O cores can, therefore, be markedly affected by the properties of the supporting ligands such as topology, denticity, and sterics, as well as the nature of the variable *cis* or *trans* ligands and the spin states of the metal center. Whereas OAT reactions will be solely controlled by the M^n=O/M^{n-1}=O reduction potentials, additional factors such as the basicity of the M=O bond as

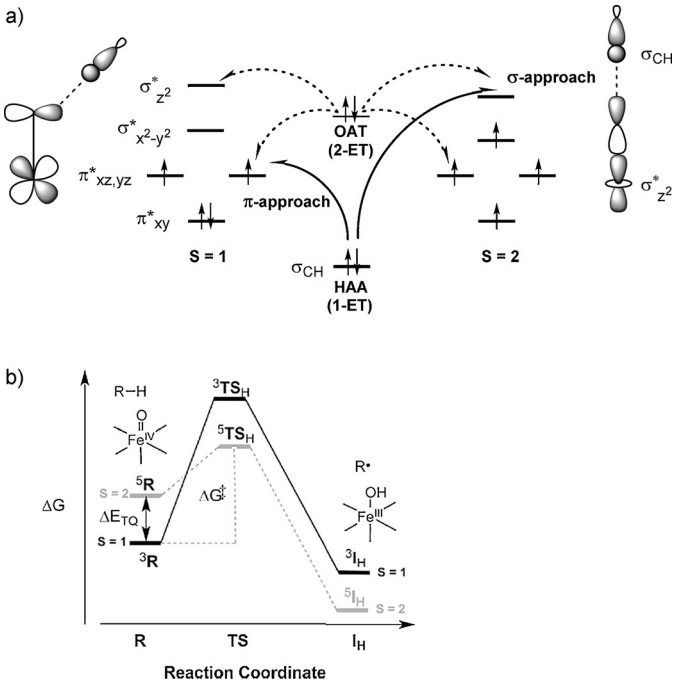

Figure 2. a) Comparison of the FMOs involved in the single-electron transfer (1-ET) HAA (solid arrows; π and σ approach) and two-electron transfer (2-ET) OAT (dashed arrows) processes carried out by Fe^{IV}=O complexes on $S=1$ and $S=2$ surfaces; b) Representation of the TSR scenario during the HAA reactions of an Fe^{IV}=O complex in a tetragonal geometry. Adapted from Ref. [31a] with permission. Copyright 2015 American Chemical Society.

well as the nature of the electron acceptor orbital will also contribute to the HAA reactivity.

In addition to the effects of supporting and axial ligands, the presence of redox-inactive metal ions (E^+) and protons (H^+) may also result in remarkable changes in the chemical properties of the M^n=O complexes.[17] The difference in reactivity may be ascribed to the positive shift of the M^n=O/M^{n-1}=O reduction potential because of the stronger binding of the E^+/H^+ ions to the more basic oxo group of the one-electron-reduced M^{n-1}=O complex; this may result in a change in the mechanism from concerted or coupled HAA or OAT reactions (in the absence of E^+/H^+) to uncoupled electron transfer (MCET or PCET) and proton transfer (PT) steps (Scheme 1).

2.1. Iron-Oxo Complexes

High-valent non-heme high-spin ($S=2$) oxoiron(IV) intermediates have been identified by means of various spectroscopic techniques as active oxidizing species in the catalytic cycles of taurine:α-ketoglutaratedioxygenase (TauD) from *E. coli*,[21] propyl-4-hydroxylase,[22] halogenase CytC3,[23] tyrosine hydroxylase,[24] and aliphatic halogenase SyrB2.[25] These reactive intermediates functionalize C–H bonds in a wide number of substrates, transforming them into hydroxylated, unsaturated, or halogenated products.[21b,22–24,26] The interesting chemistry that is exhibited by non-heme iron enzymes has inspired extensive efforts to mimic their high-valent intermediates and emulate their reactivities.[9a–c,27] Over the past decade, several non-heme oxoiron(IV) complexes with a wide range of pentadentate and tetradentate ligands have been prepared.[9a–c,27] Although, the majority of synthesized oxoiron(IV) cores have $S=1$ ground states, recent synthetic efforts have led to the stabilization of five $S=2$ oxoiron(IV) units[28] by enforcing a C_3 symmetry about the iron(IV) center (Scheme 2).

Calculations have predicted the $S=2$ Fe^{IV}=O units (electronic configuration: $d_{xy,x^2-y^2}{}^2\ d_{xz,yz}{}^2\ d_{z^2}{}^0$; Figure 2a) to be much more reactive toward C–H abstraction than their $S=1$ (electronic configuration: $d_{xy}{}^2\ d_{xz,yz}{}^2\ d_{x^2-y^2}{}^0\ d_{z^2}{}^0$; Figure 2a) counterparts.[29] The single-electron transfer in a HAA reaction on the $S=2$ surface yields a linear transition state involving a σ attack of the substrate FMO with the d_{z^2} σ* orbital, as well as limited steric interactions between the substrate and the Fe=O cores. This yields a lower steric contribution to the barrier at the transition state for the $S=2$ surface. Conversely, reactivity on the $S=1$ surface requires π attack of the substrate FMO with the $d_{xz,yz}$ π* orbital and, therefore, a side-on approach of the substrate. This results in large steric interactions between the substrate and the equatorial chelating ligands and produces a large barrier at the transition state. Furthermore, the transfer of an electron into the empty d_{z^2} orbital results in a large increase in the number of exchange interactions, which lowers the quintet barrier relative to its triplet counterpart.[29b] These two factors have been proposed to make a high-spin $S=2$ complex more reactive than the corresponding intermediate-spin $S=1$ species.[29b,c,f]

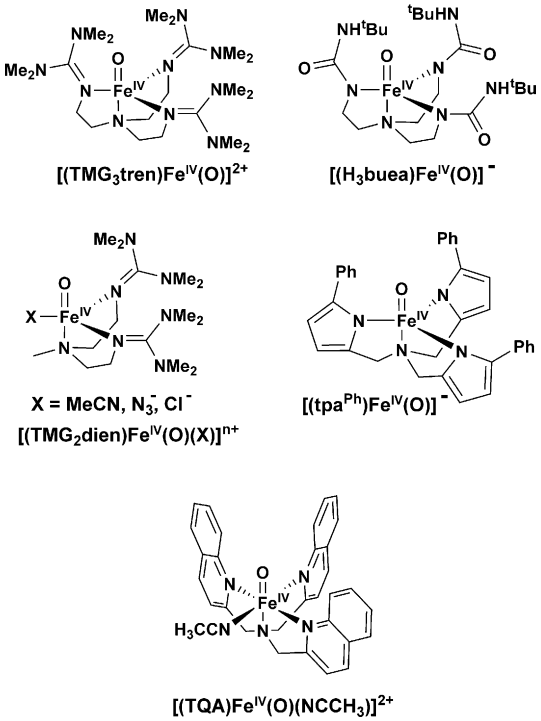

Scheme 2. Examples of biomimetic S=2 oxoiron(IV) units stabilized by enforcing a C_3 symmetry about the iron(IV) center.

The theoretically predicted activation barriers[30] as well as the kinetic isotope effects (KIEs)[30b] for HAA reactions on the triplet surface are, however, found to be inconsistent with the experimentally observed reactivity trends of the $S=1$ oxoiron(IV) model complexes. Accordingly, a two-state-reactivity (TSR) model was put forward by Shaik and co-workers to rationalize the differences in reactivity among various $S=1$ oxoiron(IV) complexes (Figure 2b).[29d,g,31a] This model postulates that the net activation barrier for cleavage of a C–H bond by intermediate-spin oxoiron(IV) complexes represents a weighted blend of the barrier on the ground triplet and excited quintet surfaces. Given that the transition state on the quintet surface lies lower than that on the triplet ground state,[29b] decreasing the triplet–quintet gap (ΔE_{TQ}) increases the accessibility of the quintet state, which, in turn, lowers the net barrier for cleavage of a C–H bond (Figure 2b). Thus, ligand-field effects that decrease ΔE_{TQ} are predicted to increase the rate of C–H bond cleavage by $S=1$ oxoiron(IV) complexes.

2.1.1. $S=1$ Oxoiron(IV) Complexes

2.1.1.1. Effect of Axial Ligands

Many studies on $[(TMC)Fe^{IV}(O)(NCCH_3)]^{2+}$ (TMC = 1,4,8,11-tetramethyl-1,4,8,11-tetraazacyclotetradecane; Figure 3a) and related chemical systems have been performed since its first characterization by X-ray and spectroscopic methods.[32] In particular, because of the fact that the sixth ligand ($NCCH_3$) is easily replaced by other ligands, this model has become the template for studies on the effect of non-heme-containing axial ligands.[33]

A contrasting reactivity pattern was established when the axially bound $NCCH_3$ ligand was substituted by anions and the reactivities of the resultant oxoiron(IV) complexes bearing different axial ligands ($[(TMC)Fe^{IV}(O)(X)]^{n+}$; X = $NCCH_3$, CF_3COO^-, N_3^-, and RS^-; Figure 3a) were investigated in terms of oxo transfer and hydrogen atom abstraction reactions (Figure 3a; Table 1, entries 1–4).[33c] While the reactivity rates of OAT to PPh_3 were found to decrease in the order $NCCH_3 > O_2CCF_3 > N_3 > SR$, consistent with the decreasing electrophilicity of the Fe=O unit, the rates of hydrogen atom abstraction from dihydroanthracene (DHA; bond dissociation energy (BDE) = 78 kcal mol^{-1}) and cyclohexadiene (CHD; BDE = 77 kcal mol^{-1}), however, increased on the introduction of a more-electron-donating axial ligand. The latter counterintuitive antielectrophilic trend, however, did not hold up upon expanding the series of $[(TMC)Fe^{IV}(O)(X)]^{n+}$ complexes to include the subsequently characterized $[(TMC_{(CH_2CONMe_2)})Fe^{IV}(O)]^{2+}$ and the conjugate base $[(TMC_{(CH=C(O^-)NMe_2)})Fe^{IV}(O)]^{+}$ (Figure 3a; Table 1, entries 5 and 6).[34] Although the linear correlation between the OAT rates and the electrophilicity of the Fe=O unit remains valid, a comparison of the HAA reactivity of the $[(TMC)Fe^{IV}(O)(NCCH_3)]^{2+}$, $[(TMC_{(CH_2CONMe_2)})Fe^{IV}(O)]^{2+}$, and $[(TMC_{(CH=C(O^-)NMe_2)})Fe^{IV}(O)]^{+}$ complexes revealed an electrophilic trend, very similar to the OAT reactivity (Figure 3a).[34]

The reactivity of the $[(TMC)Fe^{IV}(O)(X)]^{n+}$ complexes bearing different *trans* ligands can be explained on the basis of

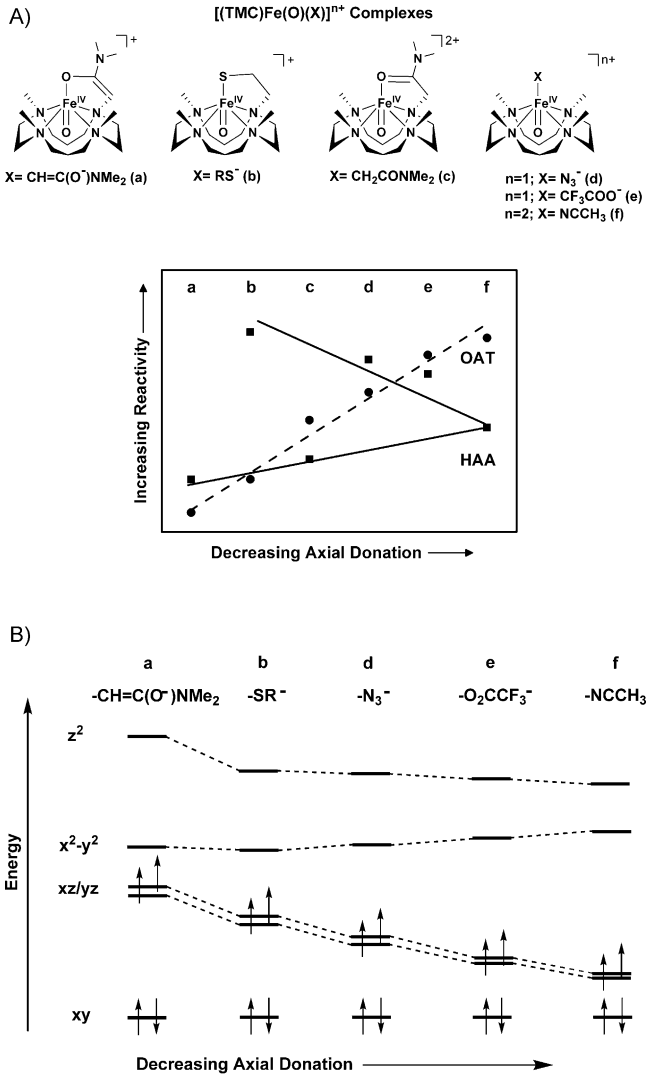

Figure 3. Axial ligand effects A) on the oxo-transfer (-----) and hydrogen-atom abstraction (——) reactivities and B) on the splitting of the 3d levels for a series of $[(TMC)Fe^{IV}(O)(X)]^{2+/+}$ complexes with various axial donations.

the modulation of the energies of the Fe=O σ* and π* antibonding molecular orbitals by the *trans* ligands. DFT calculations [33b] have revealed that the substitution of the CH_3CN ligand by an anion leads in all cases to destabilization of the d_{z^2} and $d_{xz,yz}$ orbitals (Figure 3b), and stabilization of the $d_{x^2-y^2}$ orbital. The reactivity trend of the $[(TMC)Fe^{IV}(O)(X)]^{n+}$ complexes in HAA reactions, therefore, reflects the interplay of two factors:

a) Decrease in the calculated energy gap (ΔE_{TQ}) between the triplet ground state and the quintet excited state (as evident from the stabilization of the $d_{x^2-y^2}$ orbital relative to d_{xy} as the axial ligand becomes more electron donating, thereby making the more-reactive $S=2$ state more accessible).
b) Increase in the classical activation barrier for the HAA reaction at the $S=2$ surface as a result of the increase in the energy of the d_{z^2} σ* FMO (Figure 3b).

Table 1: HAA and OAT reactivities of various metal–oxo complexes.

Entry	Complexes	T [°C]	DHA k_2 [$M^{-1}s^{-1}$]	CHD k_2 [$M^{-1}s^{-1}$]	PhEt k_2 [$M^{-1}s^{-1}$]	c-C_6H_{12} k_2 [$M^{-1}s^{-1}$]	PPh_3 k_2 [$M^{-1}s^{-1}$]	PhSMe k_2 [$M^{-1}s^{-1}$]	Ref.
	Oxoiron(IV) Complexes								
1	$[(TMC)Fe^{IV}(O)(NCCH_3)]^{2+}$	15			9.6×10^{-5}			0.012	[30a, 31a] [33c]
		0	0.14	0.12			5.9		
		−40	2.5×10^{-3}	6.4×10^{-4}					
2	$[(TMC)Fe^{IV}(O)(CF_3COO)]^{+}$	0	1.3	1.2			2.9		[33c]
3	$[(TMC)Fe^{IV}(O)(N_3)]^{+}$	0	2.4	1.4			0.61		[33c]
4	$[(TMC)Fe^{IV}(O)(RS)]^{+}$	0	7.5				0.016		[33c]
5	$[(TMC_{(CH_2CONMe_2)})Fe^{IV}(O)]^{2+}$	0		0.037			0.19		[34]
6	$[(TMC_{(CH=C(O^-)NMe_2)})Fe^{IV}(O)]^{+}$	0		0.016			<0.004		[34]
7	$[(TBC)Fe^{IV}(O)(NCCH_3)]^{2+}$	15			0.015			2.0	[30a, 31a]
8	$[(N_4Py)Fe^{IV}(O)]^{2+}$	25	18		4.0×10^{-3}	5.5×10^{-5}			[30a, 31a, 36a, 40]
		15			1.3×10^{-3}			0.33	
		−10						0.014	
		−40		0.07				2.4×10^{-4}	
9	$[(Bn\text{-}TPEN)Fe^{IV}(O)]^{2+}$	25	100		0.069	3.9×10^{-4}			[31a, 36a, 46]
		−10						0.33	
		−40		0.96				0.014	
10	$[(^{Me_2}TACN\text{-}Py_2)Fe^{IV}(O)]^{2+}$	25	7.4						[31a, 36a]
		−10						0.004	
		−40		0.027					
11	$[(BP1)Fe^{IV}(O)]^{2+}$	25	1.1						[31a,b]
		−10						0.024	
		−40		0.014					
12	$[(BP2)Fe^{IV}(O)]^{2+}$	25	40						[31a, 36a]
		−10						2.4	
		−40		0.37					
13	$[(N_3Py\text{-}(NMB))Fe^{IV}(O)]^{2+}$	25			7.6×10^{-3}	0.3×10^{-3}			[36b]
		−30						0.033	
14	$[(N_2Py\text{-}(NMB)_2)Fe^{IV}(O)]^{2+}$	25			48×10^{-3}	2.9×10^{-3}			[36b]
		−30						0.31	
15	$[(Me_3NTB)Fe^{IV}(O)]^{2+}$	−40	3.1×10^{3}	9.4×10^{2}	1.5	0.25		2.1×10^{4}	[31a, 40]
16	$[(TPA)Fe^{IV}(O)(NCCH_3)]^{2+}$	−30	4.8		5.4×10^{-3}				[31a,c,d]
17	$[(TMG_3tren)Fe^{IV}(O)]^{2+}$	−30	9.0×10^{-2}	1.2					[28a, 31a]
18	$[(TMG_2dien)Fe^{IV}(O)]^{2+}$	−30	57	18					[28b, 31a]
19	$[(TQA)Fe^{IV}(O)(NCCH_3)]^{2+}$	−40			2.1	0.37			[28c, 31a]
	Oxoiron(V) Complexes								
20	$[(TAML)Fe^{V}(O)]^{-}$	−40	230		0.145				[41b]
21	$[(TAML^*)Fe^{V}(O)]^{-}$	25			0.28	0.023			[41a]
22	$[(PyNMe_3)Fe^{V}(O)(CH_3COO)]^{2+}$	−40				2.8			[47c]
	Oxomanganese(III/IV) Complexes								
23	$[(N_4Py)Mn^{IV}(O)]^{2+}$	25	8.9	6.2	4.4×10^{-3}			9.2×10^{-3}	[55f,h, 56b]
24	$[(N_4Py)Mn^{IV}(O)Sc_2(OTf)_6]^{2+}$	0		3.5×10^{-2}				20	[55f,h]
25	$[(N_4Py)Mn^{IV}(O)(HOTf)_2]^{2+}$	25		0.92				5.9×10^{3}	[55h]
26	$[(Bn\text{-}TPEN)Mn^{IV}(O)(HOTf)_2]^{2+}$	0						3.3×10^{3}	[55h]
27	$[(Bn\text{-}TPEN)Mn^{IV}(O)]^{2+}$	25			2.7×10^{-2}			1.3	[54b, 55e]
28	$[(BQCN)Mn^{IV}(O)]^{2+}$	0	0.12	0.076					[55d]
29	$[(BP1)Mn^{IV}(O)]^{2+}$	5						0.12	[38]
30	$[(BP2)Mn^{IV}(O)]^{2+}$	5						0.012	[38]
31	$[(H_3buea)Mn^{IV}(O)]^{-}$	20	0.026						[55k]
32	$[(H_3buea)Mn^{III}(O)]^{2-}$	20	0.480						[55k]
	Hydroxo(imido)copper(III) Complexes								
33	$[(L)Cu^{III}OH]$	−25	50			2.64×10^{-5}			[68b]
34	$[(L)Cu^{II}(NTs^{\bullet})Sc(OTf)_3]^{+}$	−90	0.21	0.16			0.19		[65]
35	$[(L)Cu^{II}(NMes^{\bullet})Sc(OTf)_3]^{+}$	−90		0.030			2.89		[65b]

Whereas the former should lead to enhanced HAA reaction rates, the latter would lead to a diminished reactivity. Very recently Shaik and co-workers[30b] have shown that the effect of a smaller ΔE_{TQ} value in the $[(TMC)Fe^{IV}(O)(X)]^{n+}$ ($X = NCCH_3$, CF_3COO^-, N_3^-, and RS^-) series plays the dominant role in controlling the reactivity; as the axial donation increases, the $S=1$ Fe=O core tunnels more efficiently into the $S=2$ transition state, thereby compensating for the increase in the classical activation barrier and revealing an antielectrophilic trend in the HAA reaction. In contrast, although the tunneling contribution is significant for the $[(TMC_{(CH_2CONMe_2)})Fe^{IV}(O)]^{2+}$ and $[(TMC_{(CH=C(O^-)NMe_2)})Fe^{IV}(O)]^{+}$ complexes, it is still not sufficiently large to compensate for the large effective activation barrier resulting from the destabilization of the d_{z^2} σ* FMO in going from $[(TMC)Fe^{IV}(O)(NCCH_3)]^{2+}$ to $[(TMC_{(CH_2CONMe_2)})Fe^{IV}(O)]^{2+}$ and to $[(TMC_{(CH=C(O^-)NMe_2)})Fe^{IV}(O)]^{+}$; this results in relative HAA reaction rates of $[(TMC)Fe^{IV}(O)(NCCH_3)]^{2+} > [(TMC_{(CH_2CONMe_2)})Fe^{IV}(O)]^{2+} > [(TMC_{(CH=C(O^-)NMe_2)})Fe^{IV}(O)]^{+}$, which follows the electrophilicity of the Fe=O core.

The OAT reactions mediated by the iron-oxo complexes have been found to parallel the trends in the electrophilicity of the Fe=O core in all but one case. Que and co-workers have carried out a study with a series of $S=1$ $[(L^1Py_2)Fe^{IV}(O)(L^2)]^{2+}$ (Figure 4) complexes, where the supporting L^1Py_2 ligand provided an equatorial array of four nitrogen donors and L^2 corresponds to an axial pyridine *N*-oxide donor with various substituents at the 4-position.[35] Surprisingly, in the set of OAT experiments with diphenylsulfide as the substrate, the oxidation rates accelerated with more-electron-donating substituents, corresponding to a Hammett ρ value of −1.3 (Figure 4), which is in contrast to the electrophilic trend found for OAT reactions of the $[(TMC)Fe^{IV}(O)(X)]^{n+}$ series (Figure 3a). This may imply a change in the mechanism from a concerted two-electron OAT to a stepwise electron-transfer mechanism, so that the rate of the reaction will now depend on the nature of the FMO taking part in the initial electron-transfer reaction, very similar to HAA. Indeed, comparable Hamett ρ values for HAA (−1.4) and OAT (−1.3) reactions mediated by the $[(L^1Py_2)Fe^{IV}(O)(L^2)]^{2+}$ complexes may suggest similar rate-determining steps (i.e. electron transfer to the d_{z^2} σ* FMO on the excited $S=2$ surface) in the two cases. Such a TSR model for OAT is, however, yet to be confirmed by theoretical methods.

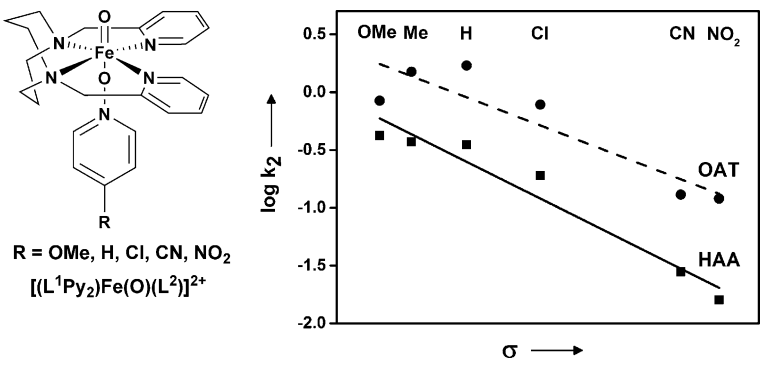

Figure 4. Hammett plots for the oxidation of benzyl alcohol (——, HAA) and diphenylsulfide (-----, OAT) by $[(L^1Py_2)Fe^{IV}(O)(L^2)]^{2+}$.

2.1.1.2. *Effect of Equatorial Ligands*

The nature of the equatorial ligands can also have a profound effect on the redox potentials and on the reactivity of the oxoiron(IV) complexes. Strong equatorial donation would lead to a lowered Fe^{IV}=O/Fe^{III}=O potential and destabilization of the $d_{x^2-y^2}$ orbital relative to d_{xy}, as reflected by the blue-shift of the λ_{max} of the near-IR spectral Fe^{IV}=O signature of the complexes.[29a,36] This shift will result in a higher ΔE_{TQ} value, and hence a lower HAA rate as a result of the lower accessibility of the more-reactive $S=2$ state. This is nicely demonstrated in the chemical properties of a series of oxoiron(IV) complexes $[(L)Fe^{IV}(O)]^{2+}$ (L = N4Py, Bn-TPEN, ^{Me_2}TACN-Py_2, BP1, and BP2; see Figure 5) of pentadentate ligands containing one tertiary amine ligand *trans* to the oxo group, and various numbers of equatorial pyridine and tertiary amine donors.[36a] Thus, the ligands differ only with respect to the extent of equatorial donation from the ligands to the Fe centers, which results in a difference of 0.3–0.4 V in the Fe^{III}–OH/Fe^{IV}=O potentials for the complexes in the series, as determined by spectropotentiometric titration methods. The main difference between the three complexes with low Fe^{III}–OH/Fe^{IV}=O potentials (i.e. for N4Py (0.90 V), ^{Me_2}TACN-Py_2 (0.83 V), and BP1(0.98 V)) and the two with the highest potentials (i.e. Bn-TPEN (1.07 V) and BP2 (1.23 V); all potentials versus Fc/Fc^+ in $NCCH_3$ containing 0.1 M water at 25 °C)[36a] is the presence of at least one pyridine donor (highlighted in gray; Figure 5) whose plane is oriented perpendicular to the Fe=O unit.

In fact, the BP2 complex has two such pyridine donors perpendicular to the Fe=O unit and exhibits the highest potential among the complexes in the series. In contrast, the BP1 complex, which is an isomer of the BP2 complex with no perpendicular pyridine rings, has a considerably lower potential that is comparable to those of the N4Py and ^{Me_2}TACN-Py_2 complexes. In an earlier DFT study on the possible isomers of Bn-TPEN, a greater instability of isomers with a larger number of perpendicular pyridine donors was noted,[37] a notion supported by the experimental observation of the lower thermodynamic stability of BP2.[36a] The difference in stability has been attributed to steric effects of the α-H atom on the perpendicular pyridine donor, which results in a weaker equatorial donation. Comparison of the OAT reaction rates of the $[(L)Fe^{IV}(O)]^{2+}$ series revealed an excellent positive correlation for the plot of $\log k_2$(OAT) values versus Fe^{III}–OH/Fe^{IV}=O potentials, where the OAT rates increased as the electrophilicity of Fe=O increased (Figure 5A, -----; Table 1, entries 8–12).

In contrast to the antielectrophilic trend observed for the $[(TMC)Fe^{IV}(O)(X)]^{n+}$ series, the HAA rates of the $[(L)Fe^{IV}(O)]^{2+}$ complexes increase as the electrophilicity of the Fe=O core increases, although the correlation is not as good as that found for the OAT rates (Figure 5B, ——; Table 1, entries 8–12). It was suggested that the downshift in the rates seen for the BP1/BP2 subset may be associated with constraints imposed by the bicyclic framework of the bispidine ligands, a pro-

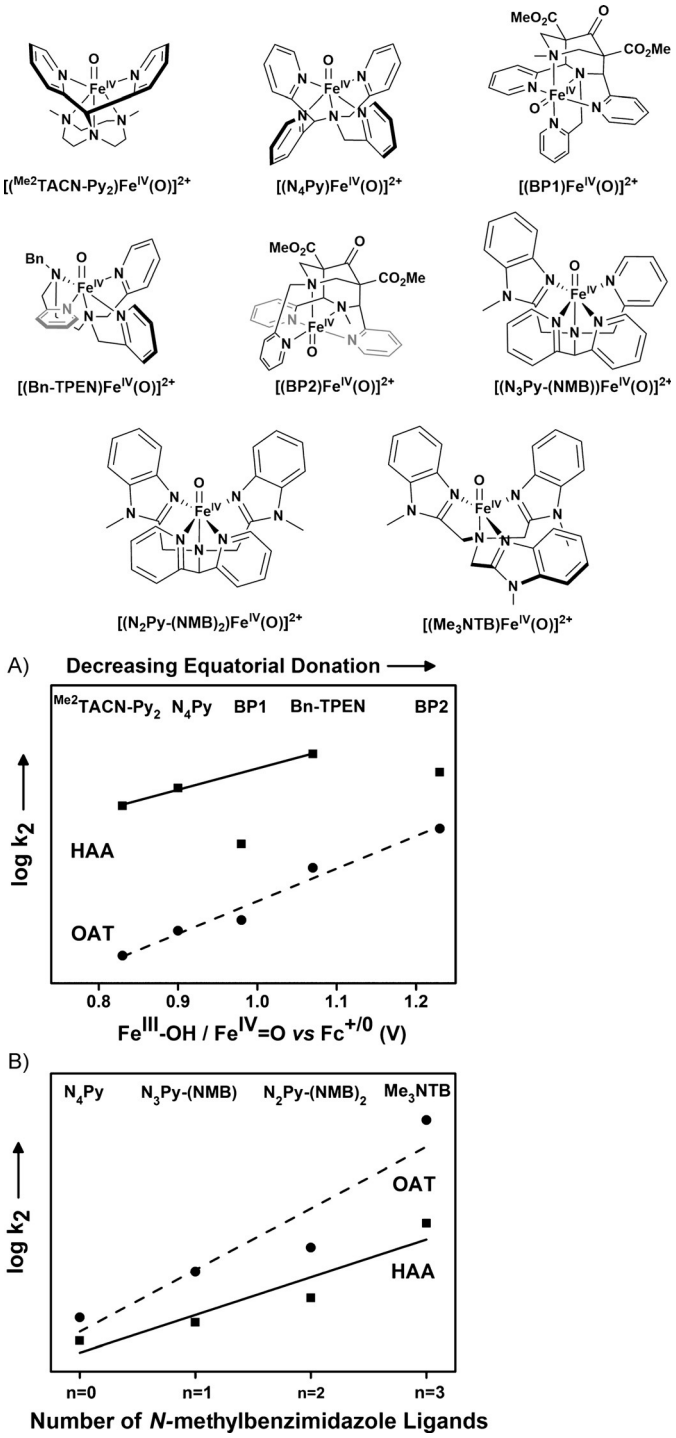

Figure 5. Effect of equatorial ligands on the reactivity of oxoiron(IV) complexes: A) Plots of the logarithms of the second-order rate constants (logk_2) for the OAT (-----; PhSMe at −10 °C) and HAA (——; DHA at 25 °C) reactivities in CH_3CN versus the Fe^{III}–OH/Fe^{IV}=O redox potential values measured by spectropotentiometry for a series of $[(L)Fe^{IV}(O)]^{2+}$ complexes involving pentadentate N-based supporting ligands (L) and containing various numbers of pyridine rings (gray) perpendicular to the Fe=O unit. B) Plots of the logk_2 values for OAT (-----; PhSMe at −30 °C) and HAA (——; *c*-C_6H_{12} at 25 °C) reactivities in CH_3CN versus the number of *N*-methylbenzimidazole donors in the supporting ligands for a series of oxoiron(IV) complexes.

posal which is also supported by the altered HAA rates of the corresponding Mn^{IV}=O complexes[38] stabilized by the BP1 and BP2 ligands.

An alternative strategy to increase the reactivity of the oxoiron(IV) complexes involves the replacement of the equatorial pyridine ligand with *N*-methylbenzimidazolyl substituents. The sp^2 character and the rigidity of this substituent should enforce a higher steric demand in the equatorial plane than that by the α-H substituent on the perpendicular pyridine donors.[39] On the other hand, the relative donor capacities of pyridine and benzimidazole can be estimated to be very similar by comparing the pK_a values of their conjugate acids (5.22 for pyridine and 5.41 for benzimidazole). Accordingly, in the oxidation of cyclohexane (*c*-C_6H_{12}; Figure 5B, ——; Table 1, entries 8, 13, and 14) and phenylmethylsulfide (PhSMe; Figure 5B, -----; Table 1, entries 8, 13, and 14), the successive replacement of pyridyl moieties of the N4Py ligand by one and two *N*-methylbenzimidazolyl moieties led to an increase of one order of magnitude in the corresponding values for the rate constants for each pyridine-donor replacement. Similarly, $[(Me_3NTB)Fe^{IV}(O)]^{2+}$ exhibits the highest oxidation rate of *c*-C_6H_{12} (and PhSMe) for any $S=1$ oxoiron(IV) complex to date (Figure 5B; Table 1, entry 15).[40] Notably, the oxidation ability of $[(Me_3NTB)Fe^{IV}(O)]^{2+}$ towards *c*-C_6H_{12} even exceeds those of the oxoiron(V) complexes $[(TAML^*)Fe^{V}(O)]^{-}$ and $[(TAML)Fe^{V}(O)]^{-}$ (TAML and TAML* are tetraamido macrocyclic ligands; Figure 6).[41a,42,47] Moreover, the HAA reactivity of $[(Me_3NTB)Fe^{IV}(O)]^{2+}$ is at least three orders of magnitude higher than that of $[(TPA)Fe^{IV}(O)(NCCH_3)]^{2+}$,[31a,c,d] (TPA = tris(2-pyridylmethyl)amine; Table 1, entry 16) and the main structural difference between the two is that $[(Me_3NTB)Fe^{IV}(O)]^{2+}$ has three benzimidazole donors instead of the pyridine groups in $[(TPA)Fe^{IV}(O)(NCCH_3)]^{2+}$. As expected, DFT calculations on $[(Me_3NTB)Fe^{IV}(O)]^{2+}$ suggest that its high reactivity is derived from a highly reactive $S=2$ excited-state surface that lies in proximity to the $S=1$ ground state.

Variations of the equatorial donation from the TMC macrocycle have also been investigated. Replacing the *N*-methyl substituents on the TMC ligand with benzyl groups to give the $S=1$ $[(TBC)Fe^{IV}(O)(NCCH_3)]^{2+}$ complex (TBC = 1,4,8,11-tetrabenzyl-1,4,8,11-tetraazacyclotetradecane) resulted in a 150-fold increase in the HAA reactivity (ethylbenzene oxidation; Table 1, entry 7),[30a] which could again be rationalized by a TSR argument. A detailed spectroscopic and computational analysis established the effect of the increased steric interactions of the benzyl groups, which distorted the cyclam ring and weakened the equatorial ligand field. This was indicated by a red-shift of the near-IR band in the absorption spectrum to 885 nm for $[(TBC)Fe^{IV}(O)(NCCH_3)]^{2+}$ relative to $[(TMC)Fe^{IV}(O)(NCCH_3)]^{2+}$ (860 nm), which presumably increased the accessibility to the more reactive quintet spin state.

2.1.1.3. *Effect of Metal Ions and Protons*

Metal ions or protons do not bind to the oxoiron(IV) unit because of the high electrophilicity of the oxygen atom. However, they bind strongly to the highly basic one-electron-

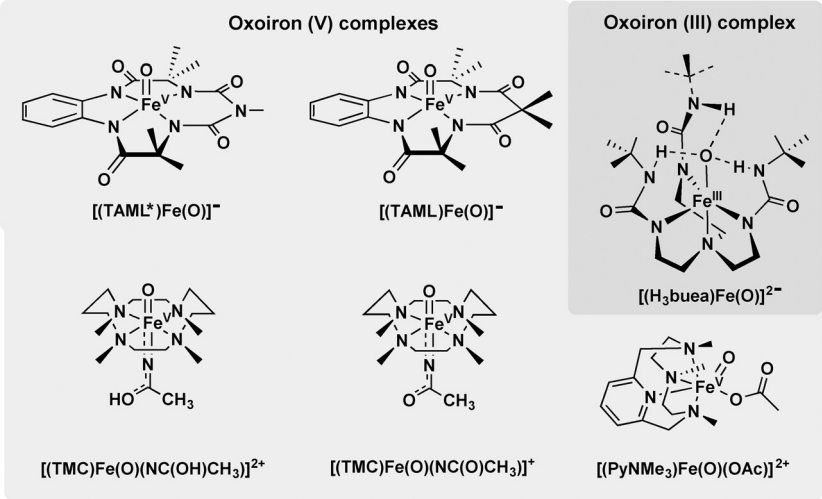

Figure 6. Known examples of complexes containing oxoiron(V) and oxoiron(III) moieties.

reduced oxoiron(III) species (Scheme 1).[43] Accordingly, the presence of metal ions or protons result in an enhancement of the reactivity of the electron-transfer reduction of the high-valent oxoiron(IV) complexes (because of the increase in the thermodynamic driving force for reduction), which is reflected in the large positive shift of the one-electron-reduction potentials (E_{red}) of the oxoiron(IV) unit.[17a,d,44] The increase in the E_{red} value also enhances the rates of the HAA or OAT reactions mediated by the oxoiron(IV) species in the presence of M^+ or H^+ ions.[45] For example, the reactivity of $[(N4Py)Fe^{IV}(O)]^{2+}$ was markedly enhanced by $HClO_4$ in the oxidation of toluene derivatives;[45e] enhancements in the rate as large as 10^3-fold from a value of $5\times10^{-2}\,M^{-1}s^{-1}$ (in the absence of $HClO_4$) to a value of $50\,M^{-1}s^{-1}$ (in the presence of 10 mM $HClO_4$) for the oxidation of hexamethylbenzene were observed. Furthermore, a significant KIE was observed when mesitylene was replaced by $[D_{12}]$mesitylene during the oxidation with $[(N4Py)Fe^{IV}(O)]^{2+}$ in CH_3CN at 298 K in the absence of $HClO_4$. This result suggests a HAA mechanism, as often observed in metal–oxo mediated C–H activation reactions.[45e] Interestingly, however, the KIE value drastically decreased from KIE = 31 in the absence of $HClO_4$ to KIE = 1.0 as the concentration of $HClO_4$ increased; this effect was accompanied by a large acceleration in the oxidation rate.[45e] The absence of a KIE suggests that the C–H oxidation of a toluene derivative occurs through a rate-determining proton-coupled electron-transfer (PCET) step in the acid-promoted oxidation reaction (Scheme 1); this is in contrast to a concerted HAA mechanism in the absence of H^+. Similarly, a metal-ion-coupled electron-transfer mechanism (MCET) prevails during the oxoiron(IV)-mediated C–H oxidation or oxo transfer reactions in the presence of M^+ ions (Scheme 1).

2.1.2. *S = 2 Oxoiron(IV) Complexes*

In contrast to the $S=1$ oxoiron(IV) complexes, the HAA reactivity of $S=2$ oxoiron(IV) complexes proceeds on a single surface and, hence, the reaction rates are controlled predominantly by the electrophilicity and steric demand of the Fe=O core. The first $S=2$ $Fe^{IV}(O)$ complex to be isolated was the trigonal-bipyramidal $[(TMG_3tren)Fe^{IV}(O)]^{2+}$ complex (Scheme 2).[28a] The HAA reactivity of this complex was found to be sluggish because of near-encapsulation of the Fe=O unit by the bulky tetramethylguanidine groups of the TMG_3tren supporting ligand that hindered electron donation to the d_{z^2} σ* FMO. Its rate of DHA (78 kcal mol^{-1}) oxidation at −30 °C was, in fact, 20-fold slower than that of the $S=1$ $[(N4Py)Fe^{IV}(O)]^{2+}$ (Table 1, entries 8 and 17), but the corresponding rates of oxidation of the smaller CHD (77 kcal mol^{-1}) were essentially identical, thus corroborating the steric access argument.[28a] The higher reactivity predicted for an $S=2$ Fe^{IV}=O moiety was, however, realized when one arm of the TMG_3tren supporting ligand was replaced by a methyl group to obtain a less sterically hindered TMG_2dien ligand (Scheme 2), and the corresponding $S=2$ $[(TMG_2dien)Fe^{IV}(O)]^{2+}$ complex was found to have a DHA oxidation rate 600-fold faster than that of $[(TMG_3tren)Fe^{IV}(O)]^{2+}$ (Table 1, entries 17 and 18).[28b] Very recently, an even more reactive $S=2$ complex, $[(TQA)Fe^{IV}(O)(NCCH_3)]^{2+}$, was obtained by substituting the highly basic guanidine donors with weaker-field quinoline ligands (Scheme 2 and Table 1, entry 19).[28c] Significantly, $[(TQA)Fe^{IV}(O)(NCCH_3)]^{2+}$ is one of the most reactive oxoiron(IV) model complexes synthesized to date. For comparison, the closely related $S=1$ $[(TPA)Fe^{IV}(O)(NCCH_3)]^{2+}$ complex does not react at all with cyclohexane at −40 °C, while the oxidation rates of cyclohexane by the $S=1$ complexes $[(N4Py)Fe^{IV}(O)]^{2+}$ and $[(Bn\text{-}TPEN)Fe^{IV}(O)]^{2+}$ at 25 °C are 3–4 orders of magnitude slower than that of $[(TQA)Fe^{IV}(O)(NCCH_3)]^{2+}$ at −40 °C, even without correcting for the 65 °C temperature difference (Table 1, entries 8, 9, and 19).[46] The observed reactivity of $[(TQA)Fe^{IV}(O)(NCCH_3)]^{2+}$ thus supports the DFT-based expectations of a more-reactive $S=2$ Fe^{IV}=O center.

2.1.3. *Oxoiron(III) and Oxoiron(V) Complexes*

In contrast to the wealth of oxoiron(IV) species, oxoiron(V)[41a,47] and oxoiron(III) species[48] (Figure 6) are quite rare. The only known example of an oxoiron(VI) species is the tetrahedral $[Fe^{VI}O_4]^{2-}$ anion derived from mineral salts.[49]] Hence, theoretical studies have been performed to understand the trends in the HAA abilities of iron-oxo complexes as a function of the iron oxidation state. For example, Neese and co-workers[50] demonstrated that the Polanyi correlation [Eq. (1)] can also be applied to rationalize the predicted electrophilic trend (the calculated reaction barrier decreased in the order $Fe^{IV} > Fe^{V} > Fe^{VI}$) in the HAA reactivities of a series of oxo-iron(IV), iron(V), and iron(VI) complexes with a nearly identical coordination geometry. Stepwise analysis, which corresponded to a successive coupling of an

electron and a proton, led to a deep understanding of the D(O-H) [Eq. (1)] trends computed for the iron-oxo series. An enhanced positive charge of a given complex resulted in an increase in the $E_{1/2}$ value and simultaneously a decrease in the pKa value; the increase in the $E_{1/2}$ value far exceeded the decrease in the pKa value, thereby making the O–H bond stronger as the oxidation state of iron increased. Consistent with the prediction of Neese and co-workers, $[(TAML)Fe^{V}(O)]^{-}$ has been found to be more reactive than the corresponding $[(TAML)Fe^{IV}(O)]^{2-}$ complexes.[51]

Furthermore, replacement of the CMe_2 group of the TAML ligand by an NMe unit in TAML* led to $[(TAML^*)Fe^{V}(O)]^{-}$, a complex that is stable at room temperature (Figure 6).[41] $[(TAML^*)Fe^{V}(O)]^{-}$ has been reported to be capable of oxidizing the strong C–H bonds of cyclohexane (BDE = 99.3 kcal mol^{-1}) at 25 °C, consistent with the theoretically predicted high HAA activity of an oxoiron(V) core. The higher thermal stability of $[(TAML^*)Fe^{V}(O)]^{-}$ relative to $[(TAML)Fe^{V}(O)]^{-}$ has been attributed to a more efficient charge delocalization in $[(TAML^*)Fe^{V}(O)]^{-}$ as a result of the presence of a planar six-membered [FeN(CO)(NMe)(CO)N] chelate ring (Figure 6).[41a] Nevertheless, the higher electron donation of the TAML* ligand results in a decrease in the $Fe^{V/IV}$ reduction potential of $[(TAML^*)Fe^{V}(O)]^{-}$ [$E_{1/2}$ in Eq. (1)], which is reflected in the demonstrated lower HAA abilities of $[(TAML^*)Fe^{V}(O)]^{-}$ relative to $[(TAML)Fe^{V}(O)]^{-}$ under comparable conditions.[41b] Subsequent replacement of the tetraanionic TAML ligand with a neutral $PyNMe_3$ ancillary ligand[47c] has further enhanced the reactivity of the oxoiron(V) core. $[(PyNMe_3)Fe^{V}(O)(CH_3COO)]^{2+}$ is the most reactive of all iron-oxo complexes known to date (Table 1, entry 22).

The C–H reactivity of the oxoiron(IV) and oxoiron(V) complexes, as evident from the above discussion, usually follows the Polanyi correlation [Eq. (1)], and gets faster as the O–H bond strength of the M^{n-1}–OH species increases. This trend is, however, not observed in the reactivity of $[(H_3buea)Fe^{III}(O)]^{2-}$ (H_3buea = tris[(*N*′-*tert*-butylureaylato)-*N*-ethylene]aminato), which represents the only example of an oxoiron(III) species known to date.[28d,48,52] Notably, $[(H_3buea)Fe^{III}(O)]^{2-}$ was found to be a stronger oxidant than the corresponding $[(H_3buea)Fe^{IV}(O)]^{-}$ complex, although the corresponding one-electron-reduced species formed by the HAA step of the former has a much lower D(O-H) value (66 kcal mol^{-1}) than that of the latter (84 kcal mol^{-1}). To help explain the puzzling reactivity of the synthetic $[(H_3buea)Fe^{III/IV}(O)]^{2-/-}$ complexes, Shaik and co-workers performed a computational study of the observed HAA reactivity. They showed that this reactivity can be attributed almost entirely to the extreme basicity of the metal–oxo unit in $[(H_3buea)Fe^{III}(O)]^{2-}$, which initiates a stepwise proton transfer followed by an electron-transfer mechanism (PT/ET; Scheme 1) for the abstraction of a hydrogen atom from a substrate.[52a] In contrast, $[(H_3buea)Fe^{IV}(O)]^{-}$ abstracts a hydrogen atom by a more traditional mechanism of near-concerted proton and electron transfer (PCET). Thus, the difference in the hydrogen-abstraction rates of the $[(H_3buea)Fe^{III/IV}(O)]^{2-/-}$ complexes mainly arises from the change in the rate-limiting step of the reactions, as the mechanism switches from concerted PCET in $[(H_3buea)Fe^{IV}(O)]^{-}$ to stepwise PT/ET in $[(H_3buea)Fe^{III}(O)]^{2-}$.

2.2. Manganese-Oxo Complexes

Non-heme manganese-oxo mediated O–O bond formation is considered to be the most critical part of the evolution of dioxygen in photosystem II.[2,10] However, the properties of a manganese-oxo center that can lead to O–O bond formation are unknown, which has led to efforts to prepare synthetic systems that probe this process. Some success has been reported, including the study by Åkermark,[53] who showed that dioxygen can be produced from oxomanganese(V) species and hydroxide ions. In addition to the oxidation of water, manganese-oxo complexes have also been invoked as oxidants in O-atom transfer reactions and the functionalization of C–H bonds.[54] However, in contrast to the well-studied non-heme iron-oxo complexes, detailed studies on manganese-oxo mediated oxidation reactions of substrates exist only for a limited number of complexes.[38,54b,55] Nevertheless, these studies have revealed some interesting differences in the properties of the manganese-oxo cores relative to the iron-oxo complexes. These will be discussed in this section.

The few known examples of mononuclear non-heme oxomanganese(IV) complexes[38,54b,55a–h] are all characterized by a $S = 3/2$ ground state with an electronic configuration of $d_{xy}^{1}d_{xz}^{1}d_{yz}^{1}d_{x^2-y^2}^{0}d_{z^2}^{0}$ in both trigonal and tetragonal ligand fields. As a consequence of the lower effective nuclear charge of Mn^{IV} relative to Fe^{IV}, the d_{z^2} orbital in oxomanganese(IV) complexes are placed higher in energy relative to those of the corresponding oxoiron(IV) complexes. Accordingly, the sterically less demanding σ pathway is energetically unfavorable for HAA reactions mediated by oxomanganese(IV) complexes, and HAA reactions proceed predominantly along a π pathway (Figure 7). Furthermore, the presence of a low-energy singly occupied d_{xy} orbital in Mn^{IV}=O provides an additional complication; for example, the transfer of an electron from a C–H bond of a substrate into the $\pi^*_{xz,yz}$ FMO (similar to that in oxoiron(IV) complexes) will lead to an unstable state, with the $\pi^*_{xz,yz}$ FMO triply occupied and the lower lying d_{xy} orbital singly occupied (Figure 7a).[56] Hence, it needs to go through an extra step of relaying the electron down to the lower orbital (Figure 7b). Alternatively, the electron in the $\pi^*_{xz,yz}$ FMO can be first excited into the $\sigma^*_{x^2-y^2}$ orbital, and then the substrate can subsequently interact with the empty π^*_{xz} orbital (Figure 7c).

The nonbonding d_{xy} and the antibonding $\sigma^*_{x^2-y^2}$ orbitals cannot directly interact with the σ(C–H) orbital as they do not have any oxygen character. It is also important to note that the d_{xy} orbital stays doubly occupied for $S = 1/2$ Mn^{IV}=O complexes, and accordingly a much lower barrier for the C–H activation reactions has been predicted on the basis of theoretical studies.[56] However, no examples of $S = 1/2$ Mn^{IV}=O complexes are known that can verify the predicted higher reactivity of the $S = 1/2$ Mn^{IV}=O state relative to the $S = 3/2$ electronic state.

Hence, as a consequence of the non-availability of the σ pathway and the additional steps involved during the

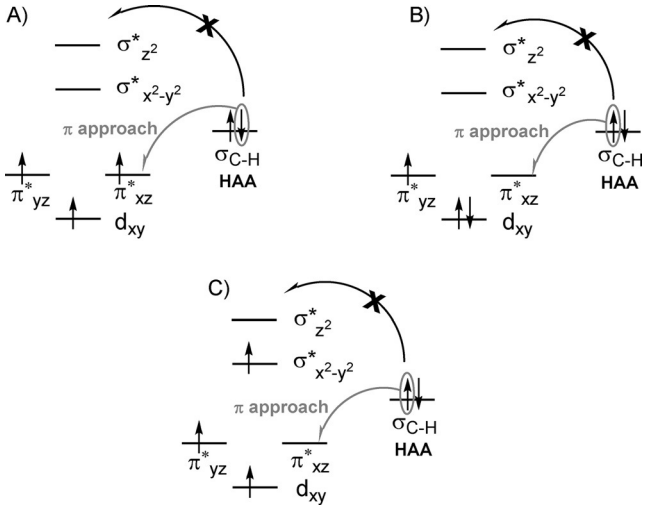

Figure 7. Comparison of the FMOs involved in the electron-transfer processes associated with the HAA reactions mediated by an oxomanganese(IV) complex on a $S=3/2$ surface. The σ pathway is unfavorable because of the high energy of the d_{z^2} orbital.

electron-transfer processes, HAA reactions are theoretically predicted to involve a higher activation barrier for Mn^{IV}=O than Fe^{IV}=O, which is also confirmed by experiment.[56b] Furthermore, HAA reactions mediated by Mn^{IV}=O species are expected to be controlled predominantly by steric effects because of the predominance of the π reactivity; this may explain the inverse reactivity pattern observed in the HAA reactivity of the Mn^{IV}=O complexes supported by the bispidine BP1 and BP2 ligands[38] relative to the Fe^{IV}=O complexes. Although the higher Fe^{IV}/Fe^{III} reduction potential of the $[(BP2)Fe^{IV}(O)]^{2+}$ complex relative to $[(BP1)Fe^{IV}(O)]^{2+}$ led to higher HAA (from an O–H bond) and OAT reactivities of the former (Table 1, entries 11 and 12; Figure 5),[36a] the corresponding $[(BP2)Mn^{IV}(O)]^{2+}$ complex was found to be less reactive than $[(BP1)Mn^{IV}(O)]^{2+}$ (Table 1, entries 29 and 30), presumably because of the higher steric demand of BP2 relative to BP1.

The higher steric requirement of the C–H oxidation reactions mediated by oxomanganese(IV) complexes is also reflected in the contrasting effect of the redox-inactive metal ions on their OAT and HAA reactivity. For example, the reactivity of the $[(N4Py)Mn^{IV}(O)]^{2+}$ complex is markedly influenced (Table 1, entries 23 and 24) by the binding of Sc^{3+} ions in oxidation reactions, such as the 2200-fold increase in the rate of oxidation of PhSMe (i.e. OAT) but a 180-fold decrease in the rate of C–H bond activation of CHD (i.e. HAA).[55f,g] A more drastic effect on the OAT reaction rate (with a rate enhancement up to 10^5 fold and an increase in the chemo- and enantioselectivity of the oxidized products) was observed in the presence of triflic acid (Table 1, entry 25).[55h,57] The enhancement of the OAT rates could be explained by the experimentally determined large positive shift in the $[Mn{=}O]^{IV/III}$ reduction potential as a result of the stronger binding of scandium ions or triflic acid to the one-electron-reduced $[Mn^{III}{=}O]$ form (Scheme 1). The deceleration of the rate of the HAA reaction was accounted for by the steric effect of the triflate counter anion or scandium triflate bound to the $[Mn^{IV}{=}O]$ form. Notably, the binding of metal ions or protons do not occur with the $[Fe^{IV}{=}O]$ form because of the higher oxo electrophilicity in $[Fe^{IV}{=}O]$ relative to that in $[Mn^{IV}{=}O]$; hence, similar steric effects were not applicable during oxidation reactions mediated by iron-oxo complexes, where the binding of metal ions resulted in the enhancement of both the OAT and HAA rates.

The basicity of the oxo groups also controls the reactivity of the Mn=O complexes.[58] Very similar to the $[(H_3buea)Fe(O)]^{2-/-}$ couple,[28d,48,52] $[(H_3buea)Mn^{III}(O)]^{2-}$ was found to be more reactive in the oxidation reactions of C–H bonds than $[(H_3buea)Mn^{IV}(O)]^{-}$ (Table 1, entries 31 and 32). The anti-electrophilic reactivity pattern has been explained (similar to that in the corresponding iron complexes) on the basis of a change in the C–H oxidation mechanism from a concerted PCET/HAA mechanism in $[(H_3buea)Mn^{IV}(O)]^{-}$ to a stepwise PT/ET process in $[(H_3buea)Mn^{III}(O)]^{2-}$.

2.3. Copper-Oxo Complexes

There is no direct evidence of mononuclear copper-oxo cores in either biological and biomimetic systems, although theoretical and model studies have supported their participation as active intermediates in various copper-mediated oxidation reactions.[59] In the absence of suitable molecular compounds containing $[CuO]^+$ cores, gas-phase reactions of isolated $[CuO]^+$ species (Scheme 3) have been employed to obtain insight into the reactivity of similar species in condensed phases.

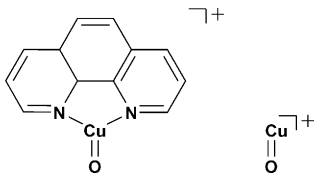

Scheme 3. Examples of isolated $[CuO]^+$ cores in the gas phase.

For example, a bare $[CuO]^+$, which, a decade ago, had already been predicted to be a powerful candidate to mediate the methane-to-methanol conversion,[61] was recently[60] generated in the gas phase and found to activate methane, with formation of 60% methanol [by an oxygen rebound mechanism; Eq. (3)] and 40% methyl radicals [through Eq. (2)]. A two-state reactivity scenario was found to be responsible for the chemoselectivity.

$$[CuO]^+ + CH_4 \rightarrow \begin{cases} [CuOH]^{\bullet +} + CH_3^{\bullet} & 40\% \quad (2) \\ [Cu]^+ + CH_3OH & 60\% \quad (3) \end{cases}$$

The HAA from methane was shown to occur more efficiently at the $[CuO]^+$ center than at the $[FeO]^+$ center, as evident from the experimentally determined lower KIE value

of 2.6 for $[CuO]^+$ versus 4.1 for $[FeO]^+$.[62] High-level quantum chemical calculations revealed that the electronic state of $[CuO]^+$ could be best represented as an open-shell $[Cu^{II}(O\cdot)]^+$ species with a triplet ($S=1$) ground state. Further detailed quantum chemical studies demonstrated the decisive role of the oxygen-centered radical in the reactivity towards methane. The preferred formation of CH_3OH is, however, the result of a subtle interplay of a two-state reactivity scenario (triplet/singlet conversion along the reaction coordinate; Figure 8) with the rather low bond energy of [Cu-O].[60,63] Notably, the importance of TSR has also been demonstrated in the reported gas-phase C–H reactivities of [(phenthroline)Cu-(O)]$^+$.[64] In contrast, theoretical studies on $[CuO]^+$-mediated aromatic hydroxylation as well as aliphatic C–H bond oxidation reactions in solution have revealed a single-state reactivity pattern, with the reactions occurring predominantly on the triplet surface.[59d,h]

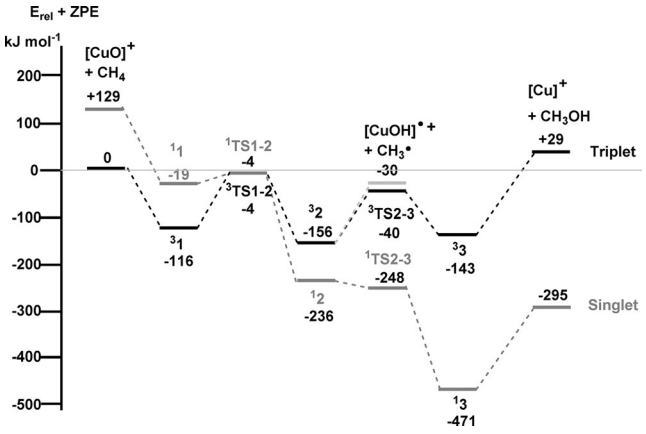

Figure 8. Potential-energy surface for the reaction of $[CuO]^+$ with CH_4 on singlet and triplet surfaces. Adapted from Ref. [60].

More direct experimental evidence that systematically shows the effect of singlet/triplet splitting energy on the reactivity of a copper-oxo species in solution is required to test the theoretically predicted reactivity patterns. Although such studies have not been possible because of the elusive nature of the copper-oxo cores in solution, related studies have been performed on copper-imido species (Figure 9),[65] which are isoelectronic to the copper-oxo core. It is important to note that metal-imido cores have often been demonstrated to exhibit chemical properties comparable to those of the corresponding metal–oxo species.[16,66] Thus, understanding the reactivity patterns of the $[Cu(NR)]^+$ core can provide detailed insights into the chemical properties of the as yet unisolated $[CuO]^+$ core. Indeed, the electronic structures of the Lewis acid stabilized $[(L)Cu(NR)]^+$ (L = 3,3-iminobis(*N*,*N*-dimethylpropylamine; R = $CH_3C_6H_4SO_2$ (Ts) or $C_6H_2(CH_3)_3$ (Mes); Figure 9)[65] have been explained on the basis of a Cu^{II} ion attached to the nitrogen-centered radical $[Cu^{II}(NR^\bullet)]^+$, which is consistent with the open-shell character

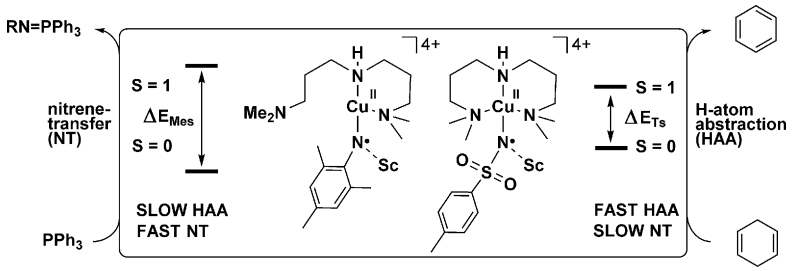

Figure 9. The reactivity properties of $[Cu(NTs)]^+$ and $[Cu(NMes)]^+$ complexes as a function of their singlet-triplet energy gaps.

predicted for the $[Cu^{II}(O^\bullet)]^+$ core in both the gas and solution phases.

Furthermore, a comparison of the HAA and nitrene transfer (NT) rates of the two complexes established some contrasting reactivity patterns, with $[Cu^{II}(NTs^\bullet)Sc(OTf)_3]^+$ (with an electron-deficient Ts substituent) being a better HAA oxidant, while $[Cu^{II}(NMes^\bullet)Sc(OTf)_3]^+$ (with an electron-donating Mes substituent) is a better NT agent (see Figure 9 and Table 1, entries 34 and 35). Notably, the lower HAA ability of $[Cu^{II}(NMes^\bullet)]^+$ is consistent with the theoretical studies on the HAA abilities of a series of $[LCu^{II}(O^\bullet)]^+$ complexes, where the HAA ability of the complexes were predicted to decrease as the electron donation from L increases.[59d] The observed differences in reactivity between $[Cu^{II}(NTs^\bullet)]^+$ and $[Cu^{II}(NMes^\bullet)]^+$ have been attributed to a five-coordinate Cu center in $[Cu^{II}(NTs^\bullet)Sc(OTf)_3]^+$, as predicted by DFT calculations, in contrast to a planar three-coordinate geometry seen in $[Cu^{II}(NMes^\bullet)Sc(OTf)_3]^+$. The Cu centers of these two complexes have different electrophilicities (Figure 9).[65b] Broken symmetry (BS) solutions were obtained for both $[Cu^{II}(NTs^\bullet)Sc(OTf)_3]^+$ and $[Cu^{II}(NMes^\bullet)Sc(OTf)_3]^+$. The calculated ground state of the latter species was an open-shell $[Cu^{II}(NMes^\bullet)]^+$ singlet with the excited triplet state lying 14.2 kcal mol^{-1} higher in energy. The calculated ground state for the complex $[Cu^{II}(NTs\cdot)Sc(OTf)_3]$ is also an open-shell singlet $[Cu^{II}(NTs^\bullet)]^+$ state; the excited BS triplet state was, however, found to be only 2.5 kcal mol^{-1} higher in energy (Figure 9). These results are, therefore, consistent with the theoretically predicted higher HAA abilities of the open-shell triplet copper-oxo unit and provide a basis for interpreting the reactivity properties of $[Cu(NR)]^+$ using a multistate reactivity model. In $[Cu^{II}(NTs^\bullet)]^+$, the triplet state with a low activation barrier for HAA is low-lying and easily accessible, which accounts for its higher HAA reactivity. The NT reaction, in contrast, proceeds predominantly on the singlet surface; the higher reactivity of $[Cu^{II}(NMes^\bullet)]^+$ can presumably be explained by the higher electrophilicity or substrate accessibility of the three-coordinate Cu center in $[Cu^{II}(NMes^\bullet)]$.

The reactivity of a $[Cu(OH)]^{2+}$ core can also provide vital insight into the reactivity of the as yet unisolated $[CuO]^+$ core. The $[Cu(OH)]^{2+}$ core has been invoked as an intermediate in water oxidation catalysis,[67] and may be viewed as a protonated form of the elusive $[CuO]^+$ unit. Tolman and co-workers very recently reported the isolation of $[LCu^{III}(OH)]$ [L = bis(2,6-diisopropylphenyl)-2,6-pyridinedicarboxamide;

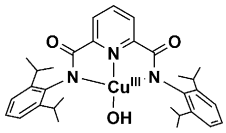

[LCu^{III}(OH)]

Scheme 4. Structure of the only known Cu^{III}–OH species.

Scheme 4] by a one-electron oxidation of the tetragonal [LCu^{II}(OH)]$^{-}$ complex at −80 °C.[13a,68] Subsequent XAS and DFT studies on [LCu^{III}-(OH)] confirmed the presence of a Cu^{III}–OH moiety. [LCu^{III}(OH)] was found to be a strong oxidant, and its ability to abstract hydrogen atoms is significantly greater than most other non-heme oxoiron(IV) complexes (Table 1, entry 33). The high reactivity of the Cu^{III}–OH species was attributed to the high basicity of the hydroxide moiety, as reflected in the determined pK_a value of 19.[13a,68] On the basis of these studies it has been speculated that a [Cu(OH)]$^{2+}$ core should be considered as an alternative in proposed mechanisms of copper-mediated oxidations by enzymes and other catalytic systems.

3. Conclusion and Perspective

The use of reactive complexes of abundant metals for synthesis, catalysis, and energy supply is of great current interest. Selective functionalization of unactivated C–H bonds in organic compounds, for example, is a highly attractive strategy in organic synthesis, and the oxidation of methane is considered one of the "Holy Grails" in synthetic chemistry.[69] Similarly, water oxidation and dioxygen reduction reactions are extremely important in the context of energy storage and utilization. A range of metalloenyzmes achieve these challenging tasks in biology by activating dioxygen and water and using cheap and abundant first-row transition metals, such as iron, copper, and manganese. Such reactions are carried out under ambient conditions with high efficiency and high stereospecificity. The recent results presented here from the bioinorganic chemistry community lend credence to the participation of high-valent metal–oxo complexes in the above-mentioned processes. A number of model metal–oxo complexes have now been synthesized and many of these complexes show intriguing reactivities, which in turn have provided vital insight into the modeled enzymatic reactions. One of the most significant conclusions from these studies is that the oxidation of strong C–H bonds, such as those of cyclohexane and *n*-butane, by synthetic $S = 2$ Fe^{IV}(O) species occurs by mechanisms reminiscent of the O_2 activation process proposed in biology. Moreover, a better understanding of the factors that control the reactivity of the iron-oxo complexes has now been achieved. It has been identified that the reactivities of high-valent metal–oxo complexes are finely controlled not only by the supporting and axial ligands but also by the binding of metal ions and protons to the metal–oxo moiety. The binding of metal ions and protons results in remarkable positive shifts in the one-electron-reduction potentials and a change in the mechanism to uncoupled electron transfer (MCET/PCET) and proton-transfer steps (Scheme 1). Furthermore, on the basis of the demonstrated high HAA ability, the [Cu(OH)]$^{2+}$ core has emerged as a possible new player in copper-mediated biological oxidation reactions of methane.

There are, nevertheless, still some gaps in our present understanding of the metal–oxo chemistry. The direct identification of copper-oxo cores in solution or the solid state has not yet been achieved, which makes their proposed involvement in biological oxidation reactions ambiguous. Moreover, the lack of any isolable metal–oxo reactive intermediates responsible for the O–O bond-formation step makes the mechanism of dioxygen evolution extremely ambiguous. Evidence in favor of the participation of the [Mn^{IV}-O$^{\bullet}$], [Fe^{V}(O)(OH)]$^{2+}$, [Fe^{V}(O)(TAML)$^{\bullet}$], [Co^{III}-O$^{\bullet}$], or [Ni^{III}-O$^{\bullet}$] cores in the O–O bond-formation step during chemical and biological water oxidation reactions is limited to theoretical studies.[9b] Thus, efforts are needed to overcome the difficulties in generating the thus-far inaccessible above-mentioned metal–oxo complexes that are of interest in the context of O–O bond-formation studies. Furthermore, the reactions exhibited by the model complexes are mostly noncatalytic, and a metal–oxo mediated methane oxidation reaction has yet to be reported. The noncatalytic behavior can be attributed to the recent finding that the activation of the C–H bond by non-heme iron(IV)-oxo and manganese(IV)-oxo complexes[17a,j] does not follow the typical hydrogen-atom abstraction/oxygen-rebound mechanism proposed in heme systems.[17k] As shown in Scheme 5, the hydroxylation of alkanes by heme systems is initiated by a rate-determining hydrogen-atom abstraction step by a [(porphyrin)$^{+\bullet}$Fe^{IV}(O)] (Cpd I) species followed by an oxygen rebound between the resulting [(porphyrin)Fe^{IV}(OH)] and substrate radical species. In this hydrogen-atom abstraction/oxygen-rebound mechanism, the Fe species with a formal oxidation state of V is reduced by two electrons to Fe^{III} and the product formed is an alcohol. The Fe^{III} product can be reoxidized to Cpd I by dioxygen activation, thereby leading to catalytic reactions. In

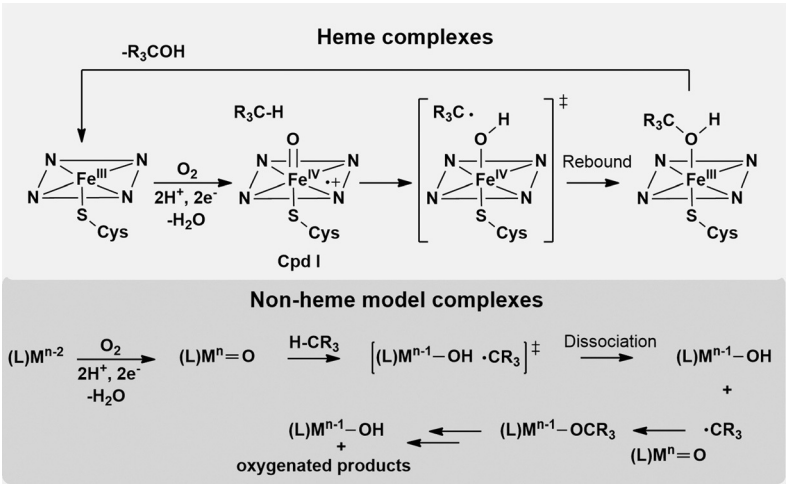

Scheme 5. Different mechanisms involved during the C–H bond-activation reactions mediated by non-heme metal–oxo model complexes.

contrast, in the case of non-heme metal–oxo model complexes, the dissociation of the substrate radical, which is formed by the abstraction of hydrogen atoms from hydrocarbons, is found to be more favorable than the oxygen-rebound processes. This gives rise to one-electron-reduced metal complexes, which can not be further oxidized to regenerate the metal–oxo species. This leads to a noncatalytic behavior. Thus, a fundamental understanding of the factors controlling the efficiency of the oxygen-rebound step in non-heme metal–oxo systems is needed to achieve catalytic C–H oxidation reactions.

The low reactivity of the model complexes can also be explained by the inability of synthetic chemists to exactly reproduce the primary metal coordination environments or the active-site structures of the metalloenzymes. Although weak-field O-donor ligands are ubiquitous in biology, most of the model compounds are based on strong-field N-rich ligands. Notably, Long's demonstration of ethane oxidation by a transient MOF-based iron-oxo core highlights the importance of an oxygen-based coordination environment in metal–oxo mediated oxidation reactions.[70] Furthermore, the unique "histidine-brace" motif that leads to a rare ligation of a primary amine to copper at the active sites of pMMO[13c,d] and LPMO[14] has only recently been reproduced in biomimetic chemistry and is proposed to play a vital role in the methane-oxidizing capability of pMMO. For example, important recent contributions from Stack and co-workers[17g,71] establish the enhanced reactivity of $Cu_2(\mu\text{-}O)_2$ cores when ligated by bidentate ligands where at least one donor is a primary amine (NH_2; Scheme 6). A combination of experimental and computational studies led to conclusions that were not obvious at the outset—the smaller size of an NH_2 function (relative to NR_2) allows for tight/strong Cu–N bonding and high valency in $Cu_2(\mu\text{-}O)_2$, without loss of oxidative power. The small NH_2 donor function also allows a closer approach of the substrate to the O_2-derived copper–oxygen species.

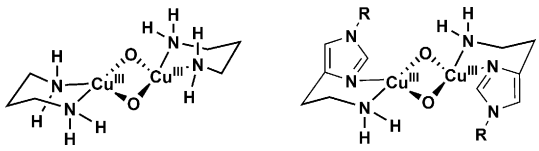

Scheme 6. Examples of $Cu_2(\mu\text{-}O)_2$ cores stabilized by ancillary ligands containing primary donors.

Interactions between metal sites and protein-derived secondary coordination spheres are also important in biocatalysis by metalloenzymes. These predominantly include a variety of noncovalent interactions between the metal center and nearby functional groups, which control the precise transfer of protons and electrons during turnover.[72] Thus, new and innovative synthetic strategies are needed to generate superoxidized metal centers in ligand environments that better resemble the active site of the metalloenzymes. These goals may eventually lead to the development of cheap and efficient bioinspired/biomimetic catalysts for dioxygen activation/reduction and water oxidation that will influence the energy landscape of our society.

Acknowledgements

We gratefully acknowledge financial support of this work from the Cluster of Excellence "Unifying Concepts in Catalysis" (EXC 314/2), Berlin. K.R. also thanks the Heisenberg-Programm of the Deutsche Forschungsgemeinschaft for financial support. I.M.-P. thanks BIG-NSE for her scholarship.

How to cite: *Angew. Chem. Int. Ed.* **2016**, *55*, 7632–7649
Angew. Chem. **2016**, *128*, 7760–7778

[1] a) M. Grätzel, *Nature* **2001**, *414*, 338–344; b) N. S. Lewis, D. G. Nocera, *Proc. Natl. Acad. Sci. USA* **2006**, *103*, 15729–15735.
[2] a) T. A. Betley, Q. Wu, T. Van Voorhis, D. G. Nocera, *Inorg. Chem.* **2008**, *47*, 1849–1861; b) S. Kundu, M. Schwalbe, K. Ray, *BioInorg. React. Mech.* **2012**, *8*, 41–57; c) J. P. McEvoy, G. W. Brudvig, *Chem. Rev.* **2006**, *106*, 4455–4483; d) N. Cox, D. A. Pantazis, F. Neese, W. Lubitz, *Acc. Chem. Res.* **2013**, *46*, 1588–1596; e) D. A. Pantazis, M. Orio, T. Petrenko, S. Zein, W. Lubitz, J. Messinger, F. Neese, *Phys. Chem. Chem. Phys.* **2009**, *11*, 6788–6798; f) N. Cox, M. Retegan, F. Neese, D. A. Pantazis, A. Boussac, W. Lubitz, *Science* **2014**, *345*, 804–808.
[3] a) L. Duan, F. Bozoglian, S. Mandal, B. Stewart, T. Privalov, A. Llobet, L. Sun, *Nat. Chem.* **2012**, *4*, 418–423; b) K. S. Joya, N. K. Subbaiyan, F. D. Souza, H. J. M. De Groot, *Angew. Chem. Int. Ed.* **2012**, *51*, 9601–9605; *Angew. Chem.* **2012**, *124*, 9739–9743; c) T. Nakagawa, C. A. Beasley, R. W. Murray, *J. Phys. Chem. C* **2009**, *113*, 12958–12961; d) L. Tong, L. Duan, Y. Xu, T. Privalov, L. Sun, *Angew. Chem. Int. Ed.* **2011**, *50*, 445–449; *Angew. Chem.* **2011**, *123*, 465–469.
[4] a) P. S. Casey, T. McAllister, K. Foger, *Ind. Eng. Chem. Res.* **1994**, *33*, 1120–1125; b) G. A. Olah, *Angew. Chem. Int. Ed.* **2005**, *44*, 2636–2639; *Angew. Chem.* **2005**, *117*, 2692–2696.
[5] R. A. Periana, D. J. Taube, S. Gamble, H. Taube, T. Satoh, H. Fujii, *Science* **1998**, *280*, 560–564.
[6] M. C. Chang, *Curr. Opin. Chem. Biol.* **2007**, *11*, 677–684.
[7] W. T. Beeson, V. V. Vu, E. A. Span, C. M. Phillips, M. A. Marletta, *Annu. Rev. Biochem.* **2015**, *84*, 923–946.
[8] K. Nagasawa, Y. Tohira, Y. Inoue, N. Tanoura, *Carbohydr. Res.* **1971**, *18*, 95–102.
[9] a) K. Ray, F. Felix, B. Wang, W. Nam, *J. Am. Chem. Soc.* **2014**, *136*, 13942–13958; b) K. Ray, F. Heims, M. Schwalbe, W. Nam, *Curr. Opin. Chem. Biol.* **2015**, *25*, 159–171; c) J. Hohenberger, K. Ray, K. Meyer, *Nat. Commun.* **2012**, *3*, 720; d) K. J. Young, B. J. Brennan, R. Tagore, G. W. Brudvig, *Acc. Chem. Res.* **2015**, *48*, 567–574.
[10] C. F. Yocum, *Coord. Chem. Rev.* **2008**, *252*, 296–305.
[11] S. K. Lee, J. C. Nesheim, J. D. Lipscomb, *J. Biol. Chem.* **1993**, *268*, 21569–21577.
[12] a) S.-K. Lee, B. G. Fox, W. A. Froland, J. D. Lipscomb, E. Münck, *J. Am. Chem. Soc.* **1993**, *115*, 6450–6451; b) L. Shu, J. C. Nesheim, K. Kauffmann, E. Münck, J. D. Lipscomb, L. Que, *Science* **1997**, *275*, 515–518; c) R. Banerjee, Y. Proshlyakov, J. D. Lipscomb, D. A. Proshlyakov, *Nature* **2015**, *518*, 431–434; d) M. H. Sazinsky, S. J. Lippard, *Acc. Chem. Res.* **2006**, *39*, 558–566; e) C. E. Tinberg, S. J. Lippard, *Acc. Chem. Res.* **2011**, *44*, 280–288.
[13] a) N. Gagnon, W. B. Tolman, *Acc. Chem. Res.* **2015**, *48*, 2126–2131; b) E. I. Solomon, D. E. Heppner, E. M. Johnston, J. W. Ginsbach, J. Cirera, M. F. Qayyum, M. T. Kieber-Emmons, C. H.

Kjaergaard, R. G. Hadt, L. Tian, *Chem. Rev.* **2014**, *114*, 3659 – 3853; c) M. A. Culpepper, G. E. Cutsail, B. M. Hoffman, A. C. Rosenzweig, *J. Am. Chem. Soc.* **2012**, *134*, 7640 – 7643; d) R. Balasubramanian, A. C. Rosenzweig, *Acc. Chem. Res.* **2007**, *40*, 573 – 580; e) C. Citek, S. Herres-Pawlis, T. D. P. Stack, *Acc. Chem. Res.* **2015**, *48*, 2424 – 2433; f) S. Itoh, *Acc. Chem. Res.* **2015**, *48*, 2066 – 2074; g) C. J. Cramer, W. B. Tolman, *Acc. Chem. Res.* **2007**, *40*, 601 – 608; h) L. Que, Jr., W. B. Tolman, *Angew. Chem. Int. Ed.* **2002**, *41*, 1114 – 1137; *Angew. Chem.* **2002**, *114*, 1160 – 1185; i) O. Bienemann, A. Hoffmann, S. Herres-Pawlis, *Rev. Inorg. Chem.* **2011**, *31*, 83 – 108; j) S. Schindler, *Eur. J. Inorg. Chem.* **2000**, 2311 – 2326; k) E. I. Solomon, J. W. Ginsbach, D. E. Heppner, M. T. Kieber-Emmons, C. H. Kjaergaard, P. J. Smeets, L. Tian, J. S. Woertink, *Faraday Discuss.* **2011**, *148*, 11 – 39; l) S. Ye, C.-Y. Geng, S. Shaik, F. Neese, *Phys. Chem. Chem. Phys.* **2013**, *15*, 8017 – 8030.

[14] S. Kim, J. Stahlberg, M. Sandgren, R. S. Paton, G. T. Beckham, *Proc. Natl. Acad. Sci. USA* **2014**, *111*, 149 – 154.

[15] a) K. Yoshizawa, N. Kihara, T. Kamachi, Y. Shiota, *Inorg. Chem.* **2006**, *45*, 3034 – 3041; b) A. Decker, E. I. Solomon, *Curr. Opin. Chem. Biol.* **2005**, *9*, 152 – 163; c) A. Crespo, M. A. Martí, A. E. Roitberg, L. M. Amzel, D. A. Estrin, *J. Am. Chem. Soc.* **2006**, *128*, 12817 – 12828.

[16] a) K. Ray, F. Heims, F. F. Pfaff, *Eur. J. Inorg. Chem.* **2013**, 3784 – 3807; b) J. Y. Lee, K. D. Karlin, *Curr. Opin. Chem. Biol.* **2015**, *25*, 184 – 193.

[17] a) W. Nam, Y.-M. Lee, S. Fukuzumi, *Acc. Chem. Res.* **2014**, *47*, 1146 – 1154; b) S. P. de Visser, J. U. Rohde, Y. M. Lee, J. Cho, W. Nam, *Coord. Chem. Rev.* **2013**, *257*, 381 – 393; c) W. Nam, *Acc. Chem. Res.* **2007**, *40*, 465 – 634; d) S. Fukuzumi, *Coord. Chem. Rev.* **2013**, *257*, 1564 – 1575; e) A. S. Borovik, *Chem. Soc. Rev.* **2011**, *40*, 1870 – 1874; f) A. Gunay, K. H. Theopold, *Chem. Rev.* **2010**, *110*, 1060 – 1081; g) C. Citek, B. Lin, T. E. Phelps, E. C. Wasinger, T. D. P. Stack, *J. Am. Chem. Soc.* **2014**, *136*, 14405 – 14408; h) S. Herres-Pawlis, R. Haase, P. Verma, A. Hoffmann, P. Kang, T. D. P. Stack, *Eur. J. Inorg. Chem.* **2015**, 5426 – 5436; i) S. Herres-Pawlis, P. Verma, R. Haase, P. Kang, C. T. Lyons, E. C. Wasinger, U. Floerke, G. Henkel, T. D. P. Stack, *J. Am. Chem. Soc.* **2009**, *131*, 1154 – 1169; j) S. Meyer, I. Klawitter, S. Demeshko, E. Bill, F. Meyer, *Angew. Chem. Int. Ed.* **2013**, *52*, 901 – 905; *Angew. Chem.* **2013**, *125*, 935 – 939; k) K. Cho, X. Wu, Y. Lee, Y. H. Kwon, S. Shaik, W. Nam, *J. Am. Chem. Soc.* **2012**, *134*, 20222 – 20225; l) J. T. Groves, G. A. McClusky, R. E. White, M. J. Coon, *Biochem. Biophys. Res. Commun.* **1978**, *81*, 154 – 160.

[18] a) P. R. Ortiz De Montellano, *Chem. Rev.* **2010**, *110*, 932 – 948; b) J. Rittle, M. T. Green, *Science* **2010**, *330*, 933 – 937; c) J. T. Groves, G. A. McCluskey, *J. Am. Chem. Soc.* **1976**, *98*, 859 – 861; d) S. Shaik, D. Kumar, S. P. de Visser, A. Altun, W. Thiel, *Chem. Rev.* **2005**, *105*, 2279 – 2328.

[19] a) J. M. Mayer, *Acc. Chem. Res.* **1998**, *31*, 441 – 450; b) G. K. Cook, J. M. Mayer, *J. Am. Chem. Soc.* **1995**, *117*, 7139 – 7156; c) K. A. Gardner, L. L. Kuehnert, J. M. Mayer, *Inorg. Chem.* **1997**, *36*, 2069 – 2078; d) C. T. Saouma, J. M. Mayer, *Chem. Sci.* **2014**, *5*, 21 – 31.

[20] a) F. G. Bordwell, J.-P. Cheng, G.-Z. Ji, A. V. Satish, X. Zhang, *J. Am. Chem. Soc.* **1991**, *113*, 9790 – 9795; b) F. G. Bordwell, M. J. Bausch, *J. Am. Chem. Soc.* **1986**, *108*, 1979 – 1985.

[21] a) J. M. Bollinger, Jr., J. C. Price, L. M. Hoffart, E. W. Barr, C. Krebs, *Eur. J. Inorg. Chem.* **2005**, 4245 – 4254; b) J. C. Price, E. W. Barr, B. Tirupati, J. M. Bollinger, Jr., C. Krebs, *Biochemistry* **2003**, *42*, 7497 – 7508.

[22] L. M. Hoffart, E. W. Barr, R. B. Guyer, J. M. Bollinger, C. Krebs, J. M. Bollinger, Jr., C. Krebs, *Proc. Natl. Acad. Sci. USA* **2006**, *103*, 14738 – 14743.

[23] D. P. Galonić, E. W. Barr, C. T. Walsh, J. M. Bollinger, C. Krebs, *Nat. Chem. Biol.* **2007**, *3*, 113 – 116.

[24] B. E. Eser, E. W. Barr, P. A. Frantom, L. Saleh, J. M. Bollinger Jr, C. Krebs, P. F. Fitzpatrick, *J. Am. Chem. Soc.* **2007**, *129*, 11334 – 11335.

[25] M. L. Matthews, C. M. Krest, E. W. Barr, F. H. Vaillancourt, C. T. Walsh, M. T. Green, C. Krebs, J. M. Bollinger, *Biochemistry* **2009**, *48*, 4331 – 4343.

[26] a) C. Krebs, D. G. Fujimori, C. T. Walsh, J. M. Bollinger, *Acc. Chem. Res.* **2007**, *40*, 484 – 492; b) D. A. Proshlyakov, T. F. Henshaw, G. R. Monterosso, M. J. Ryle, R. P. Hausinger, *J. Am. Chem. Soc.* **2004**, *126*, 1022 – 1023.

[27] a) A. R. McDonald, L. Que, *Coord. Chem. Rev.* **2013**, *257*, 414 – 428; b) W. Nam, *Acc. Chem. Res.* **2007**, *40*, 522 – 531; c) L. Que, Jr., *Acc. Chem. Res.* **2007**, *40*, 493 – 500; d) O. Y. Lyakin, A. A. Shteinman, *Kinet. Catal.* **2012**, *53*, 694 – 713.

[28] a) J. England, M. Martinho, E. R. Farquhar, J. R. Frisch, E. L. Bominaar, E. Münck, L. Que Jr., *Angew. Chem. Int. Ed.* **2009**, *48*, 3622 – 3626; *Angew. Chem.* **2009**, *121*, 3676 – 3680; b) J. England, Y. Guo, K. M. Van Heuvelen, M. A. Cranswick, G. T. Rohde, E. L. Bominaar, E. Münck, L. Que Jr., *J. Am. Chem. Soc.* **2011**, *133*, 11880 – 11883; c) A. N. Biswas, M. Puri, K. K. Meier, W. N. Oloo, G. T. Rohde, E. L. Bominaar, E. Münck, L. Que, *J. Am. Chem. Soc.* **2015**, *137*, 2428 – 2431; d) D. C. Lacy, R. Gupta, K. L. Stone, J. Greaves, J. W. Ziller, M. P. Hendrich, A. S. Borovik, *J. Am. Chem. Soc.* **2010**, *132*, 12188 – 12190; e) J. P. Bigi, W. H. Harman, B. Lassalle-Kaiser, D. M. Robles, T. A. Stich, J. Yano, R. D. Britt, C. J. Chang, *J. Am. Chem. Soc.* **2012**, *134*, 1536 – 1542.

[29] a) A. Decker, J.-U. Rohde, E. J. Klinker, S. D. Wong, L. Que Jr., E. I. Solomon, *J. Am. Chem. Soc.* **2007**, *129*, 15983 – 15996; b) S. Shaik, H. Chen, D. Janardanan, *Nat. Chem.* **2011**, *3*, 19 – 27; c) S. D. Wong, C. B. Bell, L. V. Liu, Y. Kwak, J. England, E. E. Alp, J. Zhao, L. Que, E. I. Solomon, *Angew. Chem. Int. Ed.* **2011**, *50*, 3215 – 3218; *Angew. Chem.* **2011**, *123*, 3273 – 3276; d) H. Hirao, D. Kumar, L. Que, S. Shaik, *J. Am. Chem. Soc.* **2006**, *128*, 8590 – 8606; e) M. J. Louwerse, E. Jan Baerends, *Phys. Chem. Chem. Phys.* **2007**, *9*, 156 – 166; f) M. Srnec, S. D. Wong, E. I. Solomon, *Dalton Trans.* **2014**, *43*, 17567 – 17577; g) H. Hirao, L. Que, Jr., W. Nam, S. Shaik, *Chem. Eur. J.* **2008**, *14*, 1740 – 1756; h) D. Janardanan, Y. Wang, P. Schyman, L. Que, Jr., S. Shaik, *Angew. Chem. Int. Ed.* **2010**, *49*, 3342 – 3345; *Angew. Chem.* **2010**, *122*, 3414 – 3417.

[30] a) S. A. Wilson, J. Chen, S. Hong, Y.-M. Lee, M. Clémancey, R. Garcia-Serres, T. Nomura, T. Ogura, J.-M. Latour, B. Hedman, *J. Am. Chem. Soc.* **2012**, *134*, 11791 – 11806; b) D. Mandal, R. Ramanan, D. Usharani, D. Janardanan, B. Wang, S. Shaik, *J. Am. Chem. Soc.* **2015**, *137*, 722 – 733.

[31] a) S. T. Kleespies, W. N. Oloo, A. Mukherjee, L. Que, *Inorg. Chem.* **2015**, *54*, 5053 – 5064; b) P. Comba, S. Wunderlich, *Chem. Eur. J.* **2010**, *16*, 7293 – 7299; c) G. Xue, A. Pokutsa, L. Que, *J. Am. Chem. Soc.* **2011**, *133*, 16657 – 16667; d) M. H. Lim, J.-U. Rohde, A. Stubna, M. R. Bukowski, M. Costas, R. Y. N. Ho, E. Munck, W. Nam, L. Que, *Proc. Natl. Acad. Sci. USA* **2003**, *100*, 3665 – 3670.

[32] J.-U. Rohde, J.-H. In, M. H. Lim, W. W. Brennessel, M. R. Bukowski, A. Stubna, E. Münck, W. Nam, L. Que, Jr., *Science* **2003**, *299*, 1037 – 1039.

[33] a) C. V. Sastri, M. J. Park, T. Ohta, T. A. Jackson, A. Stubna, M. S. Seo, J. Lee, J. Kim, T. Kitagawa, E. Münck, *J. Am. Chem. Soc.* **2005**, *127*, 12494 – 12495; b) T. A. Jackson, J. Rohde, M. S. Seo, C. V. Sastri, R. Dehont, A. Stubna, T. Ohta, T. Kitagawa, E. Münck, W. Nam, *J. Am. Chem. Soc.* **2008**, *130*, 12394 – 12407; c) C. V. Sastri, J. Lee, K. Oh, Y. J. Lee, T. A. Jackson, K. Ray, H. Hirao, W. Shin, J. A. Halfen, J. Kim, *Proc. Natl. Acad. Sci. USA* **2007**, *104*, 19181 – 19186; d) M. R. Bukowski, K. D. Koehntop, A. Stubna, E. L. Bominaar, J. A. Halfen, E. Münck, W. Nam, L. Que, Jr., *Science* **2005**, *310*, 1000 – 1002.

[34] J. England, J. O. Bigelow, K. M. Van Heuvelen, E. R. Farquhar, M. Martinho, K. K. Meier, J. R. Frisch, E. Münck, L. Que, *Chem. Sci.* **2014**, *5*, 1204 – 1215.

[35] Y. Zhou, X. Shan, R. Mas-Ballesté, M. R. Bukowski, A. Stubna, M. Chakrabarti, L. Slominski, J. A. Halfen, E. Münck, L. Que Jr., *Angew. Chem. Int. Ed.* **2008**, *47*, 1896 – 1899; *Angew. Chem.* **2008**, *120*, 1922 – 1925.

[36] a) D. Wang, K. Ray, M. Collins, E. Farquhar, J. R. Frisch, L. Gomez, T. A. Jackson, M. Kreschер, A. Waleska, P. Comba, *Chem. Sci.* **2013**, *4*, 282 – 291; b) M. Mitra, H. Nimir, S. Demeshko, S. S. Bhat, S. O. Malinkin, M. Haukka, J. Lloret-Fillol, G. C. Lisensky, F. Meyer, A. A. Shteinman, *Inorg. Chem.* **2015**, *54*, 7152 – 7164.

[37] E. J. Klinker, J. Kaizer, W. W. Brennessel, N. L. Woodrum, C. J. Cramer, L. Que, *Angew. Chem. Int. Ed.* **2005**, *44*, 3690 – 3694; *Angew. Chem.* **2005**, *117*, 3756 – 3760.

[38] P. Barman, A. K. Vardhaman, B. Martin, S. J. Wörner, C. V. Sastri, P. Comba, *Angew. Chem. Int. Ed.* **2015**, *54*, 2095 – 2099; *Angew. Chem.* **2015**, *127*, 2123 – 2127.

[39] M. Mitra, J. Lloret-Fillol, M. Haukka, M. Costas, E. Nordlander, *Chem. Commun.* **2014**, *50*, 1408 – 1410.

[40] M. S. Seo, N. H. Kim, K.-B. Cho, J. E. So, S. K. Park, M. Clémancey, R. Garcia-Serres, J.-M. Latour, S. Shaik, W. Nam, *Chem. Sci.* **2011**, *2*, 1039 – 1045.

[41] a) M. Ghosh, K. K. Singh, C. Panda, A. Weitz, M. P. Hendrich, T. J. Collins, B. B. Dhar, S. Sen Gupta, *J. Am. Chem. Soc.* **2014**, *136*, 9524 – 9527; b) S. Kundu, J. V. K. Thompson, L. Q. Shen, M. R. Mills, E. L. Bominaar, A. D. Ryabov, T. J. Collins, *Chem. Eur. J.* **2015**, *21*, 1803 – 1810.

[42] a) D. Dolphin, T. G. Traylor, L. Y. Xie, *Acc. Chem. Res.* **1997**, *30*, 251 – 259; b) Y. M. Goh, W. Nam, *Inorg. Chem.* **1999**, *38*, 914 – 920; c) S. R. Bell, J. T. Groves, *J. Am. Chem. Soc.* **2009**, *131*, 9640 – 9641.

[43] a) S. Fukuzumi, Y. Morimoto, H. Kotani, P. Naumov, Y.-M. Lee, W. Nam, *Nat. Chem.* **2010**, *2*, 756 – 759; b) F. Li, K. M. Van Heuvelen, K. K. Meier, L. Que, Jr., *J. Am. Chem. Soc.* **2013**, *135*, 10198 – 10201; c) M. Swart, *Chem. Commun.* **2013**, *49*, 6650 – 6652.

[44] a) Y. Morimoto, H. Kotani, J. Park, Y.-M. Lee, W. Nam, S. Fukuzumi, *J. Am. Chem. Soc.* **2011**, *133*, 403 – 405; b) S. Fukuzumi, K. Ohkubo, Y.-M. Lee, W. Nam, *Chem. Eur. J.* **2015**, *21*, 17548 – 17559.

[45] a) J. Park, Y. Morimoto, Y.-M. Lee, W. Nam, S. Fukuzumi, *Inorg. Chem.* **2014**, *53*, 3618 – 3628; b) Y. Morimoto, J. Park, T. Suenobu, Y. M. Lee, W. Nam, S. Fukuzumi, *Inorg. Chem.* **2012**, *51*, 10025 – 10036; c) J. Park, Y. Morimoto, Y. M. Lee, W. Nam, S. Fukuzumi, *J. Am. Chem. Soc.* **2011**, *133*, 5236 – 5239; d) J. Park, Y. Morimoto, Y. M. Lee, W. Nam, S. Fukuzumi, *J. Am. Chem. Soc.* **2012**, *134*, 3903 – 3911; e) J. Park, Y. M. Lee, W. Nam, S. Fukuzumi, *J. Am. Chem. Soc.* **2013**, *135*, 5052 – 5061; f) J. Park, Y.-M. Lee, K. Ohkubo, W. Nam, S. Fukuzumi, *Inorg. Chem.* **2015**, *54*, 5806 – 5812; g) Z. Chen, L. Yang, C. Choe, Z. Lv, G. Yin, *Chem. Commun.* **2015**, *51*, 1874 – 1877; h) N. C. Boaz, S. R. Bell, J. T. Groves, *J. Am. Chem. Soc.* **2015**, *137*, 2875 – 2885.

[46] J. Kaizer, E. J. Klinker, N. Y. Oh, J. U. Rohde, W. J. Song, A. Stubna, J. Kim, E. Münck, W. Nam, L. Que, *J. Am. Chem. Soc.* **2004**, *126*, 472 – 473.

[47] a) F. T. de Oliveira, A. Chanda, D. Banerjee, X. Shan, S. Mondal, L. Que, Jr., E. L. Bominaar, E. Münck, T. J. Collins, *Science* **2007**, *315*, 835 – 838; b) K. M. Van Heuvelen, A. T. Fiedler, X. Shan, R. F. De Hont, K. K. Meier, E. L. Bominaar, E. Munck, L. Que, *Proc. Natl. Acad. Sci. USA* **2012**, *109*, 11933 – 11938; c) J. Serrano-Plana, W. N. Oloo, L. Acosta-Rueda, K. K. Meier, B. Verdejo, E. García-España, M. G. Basallote, E. Münck, L. Que, Jr., A. Company, M. Costas, *J. Am. Chem. Soc.* **2015**, *137*, 15833 – 15842.

[48] C. E. MacBeth, A. P. Golombek, V. G. Young, Jr., C. Yang, K. Kuczera, M. P. Hendrich, A. S. Borovik, *Science* **2000**, *289*, 938 – 941.

[49] a) M. L. Hoppe, E. O. Schlemper, R. K. Murmann, *Acta Crystallogr. Sect. B* **1982**, *38*, 2237 – 2239; b) M. Herren, H. U. Güdel, *Inorg. Chem.* **1992**, *31*, 3683 – 3684; c) K. Wissing, M. T. Barriuso, J. A. Aramburu, M. Moreno, *J. Chem. Phys.* **1999**, *111*, 10217 – 10228; d) V. K. Sharma, L. Chen, R. Zboril, *ACS Sustainable Chem. Eng.* **2016**, *4*, 18 – 34.

[50] C. Geng, S. Ye, F. Neese, *Dalton Trans.* **2014**, *43*, 6079 – 6086.

[51] A. Chanda, X. Shan, M. Chakrabarti, W. C. Ellis, D. L. Popescu, F. Tiago de Oliveira, D. Wang, L. Que Jr., T. J. Collins, E. Münck, *Inorg. Chem.* **2008**, *47*, 3669 – 3678.

[52] a) D. Usharani, D. C. Lacy, A. S. Borovik, S. Shaik, *J. Am. Chem. Soc.* **2013**, *135*, 17090 – 17104; b) S. A. Cook, E. A. Hill, A. S. Borovik, *Biochemistry* **2015**, *54*, 4167 – 4180.

[53] Y. Gao, T. Akermark, J. Liu, L. Sun, B. Akermark, *J. Am. Chem. Soc.* **2009**, *131*, 8726 – 8727.

[54] a) J. T. Groves, J. Lee, S. S. Marla, *J. Am. Chem. Soc.* **1997**, *119*, 6269 – 6273; b) X. Wu, M. S. Seo, K. M. Davis, Y.-M. Lee, J. Chen, K.-B. Cho, Y. N. Pushkar, W. Nam, *J. Am. Chem. Soc.* **2011**, *133*, 20088 – 20091; c) R. Hage, A. Lienke, *Angew. Chem. Int. Ed.* **2005**, *45*, 206 – 222; *Angew. Chem.* **2005**, *118*, 212 – 229.

[55] a) G. Yin, *Acc. Chem. Res.* **2013**, *46*, 483 – 492; b) S. Shi, Y. Wang, A. Xu, H. Wang, D. Zhu, S. B. Roy, T. A. Jackson, D. H. Busch, G. Yin, *Angew. Chem. Int. Ed.* **2011**, *50*, 7321 – 7324; *Angew. Chem.* **2011**, *123*, 7459 – 7462; c) Y. Wang, S. Shi, H. Wang, D. Zhu, G. Yin, *Chem. Commun.* **2012**, *48*, 7832 – 7834; d) S. C. Sawant, X. Wu, J. Cho, K.-B. Bin Cho, S. H. Kim, M. S. Seo, Y.-M. M. Lee, M. Kubo, T. Ogura, S. Shaik, *Angew. Chem. Int. Ed.* **2010**, *49*, 8190 – 8194; *Angew. Chem.* **2010**, *122*, 8366 – 8370; e) D. F. Leto, R. Ingram, V. W. Day, T. A. Jackson, *Chem. Commun.* **2013**, *49*, 5378 – 5380; f) J. Chen, Y.-M. Lee, K. M. Davis, X. Wu, M. S. Seo, K.-B. Cho, H. Yoon, Y. J. Park, S. Fukuzumi, Y. N. Pushkar, *J. Am. Chem. Soc.* **2013**, *135*, 6388 – 6391; g) H. Yoon, Y.-M. Lee, X. Wu, K.-B. Cho, R. Sarangi, W. Nam, S. Fukuzumi, *J. Am. Chem. Soc.* **2013**, *135*, 9186 – 9194; h) J. Chen, H. Yoon, Y.-M. Lee, M. S. Seo, R. Sarangi, S. Fukuzumi, W. Nam, *Chem. Sci.* **2015**, *6*, 3624 – 3632; i) T. Taguchi, R. Gupta, B. Lassalle-Kaiser, D. W. Boyce, V. K. Yachandra, W. B. Tolman, J. Yano, M. P. Hendrich, A. S. Borovik, *J. Am. Chem. Soc.* **2012**, *134*, 1996 – 1999; j) R. Gupta, T. Taguchi, B. Lassalle-Kaiser, E. L. Bominaar, J. Yano, M. P. Hendrich, A. S. Borovik, *Proc. Natl. Acad. Sci. USA* **2015**, *112*, 5319; k) T. H. Parsell, M.-Y. Yang, A. S. Borovik, *J. Am. Chem. Soc.* **2009**, *131*, 2762 – 2763; l) I. Garcia-Bosch, A. Company, C. W. Cady, S. Styring, W. R. Browne, X. Ribas, M. Costas, *Angew. Chem. Int. Ed.* **2011**, *50*, 5648 – 5653; *Angew. Chem.* **2011**, *123*, 5766 – 5771.

[56] a) K. Cho, S. Shaik, W. Nam, *J. Phys. Chem. Lett.* **2012**, *3*, 2851 – 2856; b) J. Chen, K.-B. Cho, Y.-M. Lee, Y. H. Kwon, W. Nam, *Chem. Commun.* **2015**, *51*, 13094 – 13097.

[57] C. Miao, B. Wang, Y. Wang, C. Xia, Y.-M. Lee, W. Nam, W. Sun, *J. Am. Chem. Soc.* **2016**, *138*, 936—943.

[58] T. H. Parsell, R. K. Behan, M. T. Green, M. P. Hendrich, A. S. Borovik, *J. Am. Chem. Soc.* **2006**, *128*, 8728 – 8729.

[59] a) A. Crespo, M. A. Martí, A. E. Roitberg, L. M. Amzel, D. A. Estrin, *J. Am. Chem. Soc.* **2006**, *128*, 12817 – 12828; b) T. Kamachi, N. Kihara, Y. Shiota, K. Yoshizawa, *Inorg. Chem.* **2005**, *44*, 4226 – 4236; c) S. Hong, S. M. Huber, L. Gagliardi, C. C. Cramer, W. B. Tolman, *J. Am. Chem. Soc.* **2007**, *129*, 14190 – 14192; d) S. M. Huber, M. Z. Ertem, F. Aquilante, L. Gagliardi, W. B. Tolman, C. J. Cramer, *Chem. Eur. J.* **2009**, *15*, 4886 – 4895; e) P. Capdevielle, D. Sparfel, J. Baranne-Lafont, N. K. Cuong, M. Maumy, *J. Chem. Soc. Chem. Commun.* **1990**, 565 – 566; f) N. Kitajima, T. Koda, Y. Iwata, Y. Moro-oka, *J. Am. Chem. Soc.* **1990**, *112*, 8833 – 8839; g) N. Kitajima, Y. Moro-oka, *Chem. Rev.*

1994, *94*, 737 – 757; h) P. Comba, S. Knoppe, B. Martin, G. Rajaraman, C. Rolli, B. Shapiro, T. Stork, *Chem. Eur. J.* **2008**, *14*, 344 – 357; i) D. Maiti, A. A. Narducci Sarjeant, K. D. Karlin, *Inorg. Chem.* **2008**, *47*, 8736 – 8747.

[60] N. Dietl, C. Van Der Linde, M. Schlangen, M. K. Beyer, H. Schwarz, *Angew. Chem. Int. Ed.* **2011**, *50*, 4966 – 4969; *Angew. Chem.* **2011**, *123*, 5068 – 5072.

[61] Y. Shiota, K. Yoshizawa, *J. Am. Chem. Soc.* **2000**, *122*, 12317 – 12326.

[62] D. Schröder, H. Schwarz, *Angew. Chem. Int. Ed. Engl.* **1990**, *29*, 1433 – 1434; *Angew. Chem.* **1990**, *102*, 1468 – 1469.

[63] a) E. Rezabal, J. Gauss, J. M. Matxain, R. Berger, M. Diefenbach, M. C. Holthausen, *J. Chem. Phys.* **2011**, *134*, 064304; b) E. Rezabal, F. Ruipérez, J. M. Ugalde, *Phys. Chem. Chem. Phys.* **2013**, *15*, 1148 – 1153.

[64] a) D. Schröder, M. C. Holthausen, H. Schwarz, *J. Phys. Chem. B* **2004**, *108*, 14407 – 14416; b) N. J. Rijs, P. Gonzalez-Navarrete, M. Schlangen, H. Schwarz, *J. Am. Chem. Soc.* **2016**, *138*, 3125 – 3135.

[65] a) S. Kundu, E. Miceli, E. Farquhar, F. F. Pfaff, U. Kuhlmann, P. Hildebrandt, B. Braun, C. Greco, K. Ray, *J. Am. Chem. Soc.* **2012**, *134*, 14710 – 14713; b) S.-L. Abram, I. Monte-Pérez, F. F. Pfaff, E. R. Farquhar, K. Ray, *Chem. Commun.* **2014**, *50*, 9852 – 9854.

[66] a) J. F. Berry, S. D. George, F. Neese, *Phys. Chem. Chem. Phys.* **2008**, *10*, 4361 – 4374; b) P. Leeladee, D. P. Goldberg, *Inorg. Chem.* **2010**, *49*, 3083 – 3085; c) M. J. Zdilla, M. M. Abu-Omar, *J. Am. Chem. Soc.* **2006**, *128*, 16971 – 16979.

[67] a) M. K. Coggins, M.-T. Zhang, Z. Chen, N. Song, T. J. Meyer, *Angew. Chem. Int. Ed.* **2014**, *53*, 12226 – 12230; *Angew. Chem.* **2014**, *126*, 12422 – 12426; b) J. Du, Z. Chen, S. Ye, B. J. Wiley, T. J. Meyer, *Angew. Chem. Int. Ed.* **2015**, *54*, 2073 – 2078; *Angew. Chem.* **2015**, *127*, 2101 – 2106.

[68] a) P. J. Donoghue, J. Tehranchi, C. J. Cramer, R. Sarangi, E. I. Solomon, W. B. Tolman, *J. Am. Chem. Soc.* **2011**, *133*, 17602 – 17605; b) D. Dhar, W. B. Tolman, *J. Am. Chem. Soc.* **2015**, *137*, 1322 – 1329.

[69] B. A. Arndtsen, R. G. Bergman, T. A. Mobley, T. H. Peterson, *Acc. Chem. Res.* **1995**, *28*, 154 – 162.

[70] D. J. Xiao, E. D. Bloch, J. A. Mason, W. L. Queen, M. R. Hudson, N. Planas, J. Borycz, A. L. Dzubak, P. Verma, K. Lee, F. Bonino, V. Crocella, J. Yano, S. Bordiga, D. G. Truhlar, L. Gagliardi, C. M. Brown, J. R. Long, *Nat. Chem.* **2014**, *6*, 590 – 595.

[71] C. Citek, J. B. Gary, E. C. Wasinger, T. D. Stack, *J. Am. Chem. Soc.* **2015**, *137*, 6991 – 6994.

[72] a) S. A. Cook, A. S. Borovik, *Acc. Chem. Res.* **2015**, *48*, 2407 – 2414; b) N. M. Marshall, D. K. Garner, T. D. Wilson, Y.-G. Gao, H. Robinson, M. J. Nilges, Y. Lu, *Nature* **2009**, *462*, 113 – 116.

Received: January 17, 2016
Revised: March 15, 2016
Published online: June 10, 2016

